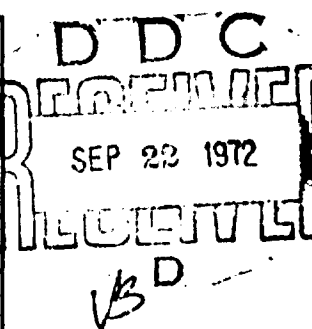
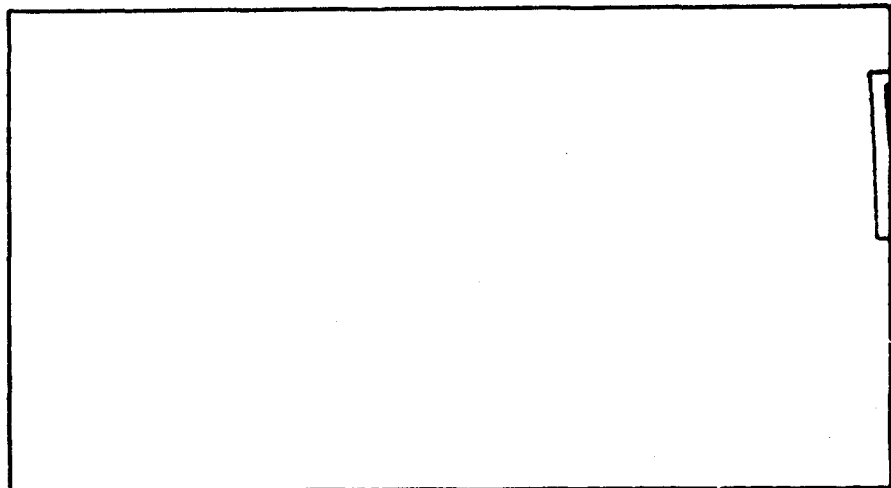


AD 748350

AIR FORCE INSTITUTE OF TECHNOLOGY



AIR UNIVERSITY
UNITED STATES AIR FORCE



SCHOOL OF ENGINEERING

Reproduced by
NATIONAL TECHNICAL
INFORMATION SERVICE
U.S. Department of Commerce
Springfield, VA 22151

WRIGHT-PATTERSON AIR FORCE BASE, OHIO

Unclassified

Security Classification

DOCUMENT CONTROL DATA - R & D

(Security classification of title, body of abstract and indexing annotation must be entered when the overall report is classified)

1. ORIGINATING ACTIVITY (Corporate author)

Air Force Institute of Technology (AFIT-EN)
Wright-Patterson AFB, Ohio 45433

2a. REPORT SECURITY CLASSIFICATION

Unclassified

2b. GROUP

3. REPORT TITLE

AN EXPERIMENTAL STUDY OF ATTENUATION OF SHOCK WAVES IN THREE MIXTURES

4. DESCRIPTIVE NOTES (Type of report and inclusive dates)

AFIT Thesis

5. AUTHOR(S) (First name, middle initial, last name)

James W. Clark, Jr.
Major, USAF

6. REPORT DATE

June 1972

7a. TOTAL NO. OF PAGES

82

7b. NO. OF REFS

12

8a. CONTRACT OR GRANT NO.

b. PROJECT NO.

c. N/A

d.

8c. ORIGINATOR'S REPORT NUMBER(S)

AFIT Thesis
GAW/MC/72-3

9d. OTHER REPORT NO(S) (Any other numbers that may be assigned to this report)

10. DISTRIBUTION STATEMENT

Approved for public release; distribution unlimited.

Approved for public release; IAW AFR 190-17-1 CENSORING MILITARY ACTIVITY
Keith A. Williams, 1st Lt., USAF
Acting Director of Information

Air Force Flight Dynamics Lab
Wright-Patterson AFB, Ohio 45433

11. ABSTRACT

Two experiments were conducted to determine the effects of adding a gas to a foam-water mixture to increase the attenuation of shock waves caused by hydraulic ram. In each experiment three target materials were impacted: water, water and reticulated polyurethane foam, and water and Pneumacel. Pneumacel is a Du Pont trademarked product consisting of Dacron fibers inflated with 12% by weight Freon gas. In the first experiment, plane (one dimensional) shock waves were generated by impacting the target materials with a flat aluminum disc. In the second experiment, $\frac{1}{2}$ in. spheres were fired into the target materials. In each experiment pressures were measured at various depths in each mixture for several impact velocities. An increase in attenuation of shock waves was observed in both experiments when foam was added to the water. Most of this increase was attributed to the presence of approximately 6% by volume of air present in the water-foam mixture. Significantly reduced pressures and increased attenuation of shock waves were observed in the water-Pneumacel (foam and gas) experiments. The results are compared to applicable theoretical models.

iB

DD FORM 1 NOV 68 1473

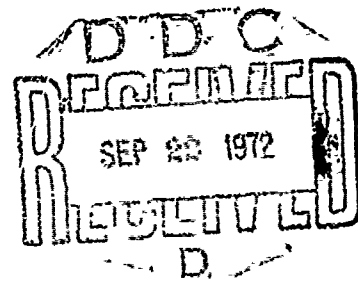
Unclassified
Security Classification

KEY WORDS	LINK A		LINK B		LINK C	
	ROLE	WT	ROLE	WT	ROLE	WT
1. Shock waves 2. Hydraulic Ram 3. Attenuation of Shock Waves 4. Impacts into Fuel Tanks 5. Porous Mixtures 6. Reticulated Polyurethane Foam 7. Fuel Cell Survivability						

AN EXPERIMENTAL STUDY OF
ATTENUATION OF SHOCK WAVES
IN THREE MIXTURES

THESIS

GAW/MC/72-3 James W. Clark, Jr.
 Major USAF



Approved for public release; distribution unlimited.

AN EXPERIMENTAL STUDY OF
ATTENUATION OF SHOCK WAVES
IN THREE MIXTURES

THESIS

Presented to the Faculty of the School of Engineering of
the Air Force Institute of Technology
Air University
in Partial Fulfillment of the
Requirements for the Degree of
Master of Science

by

James W. Clark, Jr., B. S.
Major USAF

Graduate Air Weapons

June 1972

1D

Approved for public release; distribution unlimited.

Preface

This report represents many hours of work in research, experimentation, data analysis, and manuscript preparation.	11
My sincere hope that the information contained in this report will either prove to be directly useful, or will inspire another to create technology that will be useful in area of aircraft fuel cell survivability.	iv
	vi
	vii
I wish to thank the many individuals and groups without whose effort and support this research would not have been possible. Specifically, I want to thank Dr. Peter J. Torvik, thesis advisor; Mr. Hallock F. Swift and the University Dayton Research Institute; Mr. Leavelle Mahood and the Livable Fuel Tanks Lab of the Air Force Flight Dynamics Laboratory; and Mr. Colin B. Blakemore of the Du Pont Corporation supplied part of the Pneumacel and furnished information about it. I wish also to thank Mr. Charles Gebhart for his time and help in obtaining much of the equipment used for the first part of the study, Mr. James Green for his assistance with the second part of the study, and 1/Lt. Richard Fischer for supplying additional background information report he had prepared.	1
	1
	3
	4
	6
	6
	16
	18
	18
	20
	23
	23
	36
	52
	52
	53
	54
	56
	59
	62
	71
	74

**BEST
AVAILABLE COPY**

List of Figures

Figure		Page
1	Experiment I General Apparatus Layout . . .	7
2	Impact Assembly	8
3	Experiment I Gage Location	12
4	Experiment II General Apparatus Layout . .	13
5	Experiment II Target and Gage Location . .	15
6	Visicorder Data Runs 5 and 6, water . . .	24
7	Visicorder Data Runs 7 and 8, water . . .	25
8	Visicorder Data Runs 9, 11, 12, 13, Pneumacel	26
9	Visicorder Data Runs 14, 15, 16, 17, Foam	27
10	Visicorder Data Shots 1, 2, 3, 4, water .	28
11	Visicorder Data Shots 5, 6, 7, Pneumacel.	29
12	Visicorder Data Shots 8, 9, 10, Foam . .	30
13	Visicorder Data Shots 11, 12, 13, Foam .	31
14	Visicorder Data Shots 14, 15, 16, Pneumacel.	32
15	Visicorder Data Shots 17, 18, 19, 20 water	33
16	Scope Picture Shot 13	34
17	Scope Picture Shot 14	34
18	Scope Picture Shot 15	35
19	Scope Picture Shot 17	35
20	Pressure vs Depth $\frac{1}{2}$ m drops	38
21	Pressure vs Depth 1 m drops	39
22	Pressure vs Depth $1\frac{1}{2}$ m drops	40
23	Pressure vs Depth 2 m drops	41
24	P ₀ Extrapolated vs Velocity	42

Figure	Page
25 Pressure vs Depth, Low Velocity Group . . .	46
26 Pressure vs Depth, Medium Velocity Group . .	47
27 Pressure vs Depth, High Velocity Group . . .	48
28 Pressure vs Depth, 2 m drops and Low Velocity Group	50
29 Impact Velocity vs Gage 3 Pressures	51
30 Pneumacel	58
31 Reticulated Polyurethane Foam	58
32 Pressure Calibration Apparatus	60
33 Example of a Graphical Solution of Impact Velocity for Experiment I	63

List of Tables

Table		Page
I	Curve Fit Coefficients for $P_o P_{eax}$ and Standard Error	36
II	Impact Velocity Calculations	64
III	Theoretical Calculations for Experiment I	67
IV	Mass Fraction Calculations	70
V	Tabulated Results of Experiment I . . .	72
VI	Tabulated Results of Experiment II . . .	73

Abstract

When an aircraft fuel tank is penetrated by a ballistic velocity projectile, a phenomenon known as hydraulic ram often causes the catastrophic failure of the cell. This study was performed to investigate experimentally the possibility of using porous material to defeat or significantly reduce the hydraulic ram effect. Two experiments were performed to determine how the addition of a gas to a fuel-foam mixture would affect the attenuation of shock waves and weaker pressure pulses. In the first experiment, water, water with reticulated (open cell) polyurethane foam, and water with Pneumacel (a new Du Pont product composed of Freon inflated Dacron fibers pressed into a mat) were each impacted by a flat aluminum disc to generate plane (one dimensional) shock waves in the mixtures. Four pressure transducers were located at specified distances below the surface and the attenuation of the pressure pulses in the different mixtures was measured.

In the second experiment $\frac{1}{2}$ in. spheres were fired into a tank containing, in turn, each of the three mixtures, and again the attenuation of the pressure pulses was determined. In each experiment there was an increase in attenuation noted when the reticulated foam was added to the water. However, a much greater increase was noted when the Pneumacel replaced the foam. Perhaps most interesting is the fact that pressure dropped and remained below approximately 14 psi within a few inches of the surface in all tests with Pneumacel.

I. Introduction

Background

Recent combat experience has shown that modern aircraft continue to be vulnerable to small arms fire. Aircraft fuel systems are particularly large and vulnerable areas. Within the past few years many aircraft have been modified by the installation of reticulated -(open cell) polyurethane foam in some fuel cells to decrease the probability that an empty, or partially empty, fuel cell would explode when struck by an incendiary bullet. However, both modified and unmodified fuel cells still fail catastrophically if hit when full. Even self-sealing bladders are unable to prevent massive fuel leaks when the supporting tank wall is heavily damaged.

Hydraulic Ram. Several mechanisms acting individually or in combination produce the massive damage to the fuel cell walls. These mechanisms collectively are usually called the hydraulic ram effect. Williams (Ref 11:1-4) divided the damage causing mechanism into four separate events: (1) shock waves near the impact point, (2) a pressure field caused by the passing projectile, (3) a cavity phase caused by the collapse of the cavity or void behind the projectile, and (4) impact into an adjacent wall of high velocity fuel particles ejected from a free surface by the passing projectile. In a Northrop Shock Wave Study (Ref 9) the damage causing mechanisms were divided into eight events, placing major emphasis on (1) a pressure rise when the projectile tumbles, (2) compression of the fluid as the projectile approaches

the back wall, and (3) the pressure wave preceding the large tumbling cavitation. There is little clear understanding of any of the different hydraulic ram events, and since they often occur together it is difficult to determine which one actually caused the failure in any given instance. Also the damage caused by any one mechanism appears to be a function of several variables such as fuel cell geometry, tank wall material, impact velocity, and whether or not the projectile tumbles.

Generally, attempts to defeat the hydraulic ram effects have taken one of two approaches: trial and error experiments, and analytical models. Northrop (Ref 6) used the trial and error approach to design a system to minimize tank wall damage to allow self-sealing bladders to function. However, a defense that helps in one case may not help in a different shape tank, against a different type projectile, or where a different damage causing mechanism becomes critical. Also the same approach may not protect walls other than those penetrated by the projectile.

With the analytical approach, attempts are made to predict the pressures caused by the impacting projectiles. If sufficiently accurate models can be developed, the pressure information can be used to determine structural design requirements for the fuel cells. Usually the assumption is made that one or two of the damage mechanisms are most critical and a suitable model for those mechanisms is sought. Yurkovich (Ref 12) developed a model based on a spherical shock wave, and Bristow (Ref 2) and Lundstrom (Ref 8)

have developed models for the drag or pressure phase. To date these models have not been sufficiently developed to yield the desired design information. Again, the mechanisms often occur together, and modeling of any one mechanism alone may not be sufficient.

Composite Mixture Theories. Interest in composite materials has led to the development of numerous models to predict various properties of mixtures. A model by Herrmann (Ref 7) predicted significant increases in the attenuation of shock waves in a material if small amounts of porosity were added. Torvik (Ref 10) developed a simple mixture theory for mixtures of solids or a solid and a gas. Fischer (Ref 4) applied the Torvik model and other models to varying ratios of the two mixtures: water with reticulated polyurethane foam, and water with air. In general, he found that these models predict attenuation of shock waves to be reduced as more reticulated foam is added to the mixture. Conversely, these models predict an increase in the attenuation of shock waves if increasing amounts of air are assumed to be present in the mixture. Experiments with reticulated foam have produced conflicting results. Clark (Ref 3) reported increased attenuation when polyurethane foam was added to water, while Williams (Ref 11) found pressures increased when foam was added..

Purpose and Scope

The purpose of this study was to investigate experimentally the effects on attenuation of shock waves caused by addition of a gas to a water-foam mixture. Water was used in

place of fuel for obvious safety reasons and because it allowed comparisons to be made with previous experimental and analytical studies. Since these models consider water and polyurethane foam to be "perfect" materials (having no dissipative forces) the only attenuation of shock waves calculated by models is caused by geometric dispersion of the shock front and rarefaction waves overtaking and reducing the shock waves. Because some attenuation may in fact be caused by mechanical losses, the attenuation of the shock waves in water alone was measured first. The experiments then measured the attenuation in water-foam and water-foam-gas mixtures. The study was divided into two parts: the first using plane (one dimensional) shock waves, and the second considering shock waves generated by ballistic impacts.

The first experiment was designed to study the attenuation of shock waves in water and the two mixtures under conditions which eliminated the unknowns usually introduced by the various hydraulic ram mechanisms. In the second experiment, attenuation of pressures generated by ballistic impacts were measured for the same three target materials. Spherical projectiles were used to eliminate the tumbling frequently observed with ogival projectiles.

System of Units

Most impact studies are conducted using the CGS system of units. Measurements for data in this study were made in the CGS system and results are also reported in that system. However, since standard American materials and equipment were used in the construction of the experimental apparatus,

GAW/MC/72-3

this apparatus will be described in the British system.

Additionally, the results will also be presented in British units for the convenience of those more familiar with hydraulic ram research.

II. Experimental Apparatus

Target Materials

Water was used as the first target material. The results of the tests with water formed a baseline against which the results of the mixtures were evaluated.

The second material selected was water and a reticulated polyurethane foam. This foam is currently used to fill some aircraft fuel cells to prevent explosions in empty tanks.

The third target material used was water and Pneumacel. Pneumacel is a new Du Pont tradenamed product now in pilot production and currently used in rug pads. It is a mat made of Dacron fibers inflated with approximately 12% by weight Freon gas. Pneumacel was selected because it is a sponge-like product containing controlled amounts of gas and met all other needs of the experiment.*

Apparatus

This investigation involved the use of two separate experiments, each with its own apparatus.

Experiment I. The object of the first part of the study was to generate plane (one dimensional) shock waves in the different target materials and determine the attenuation of these shock waves by measuring the pressures at specified depths in the various mixtures. The general layout of the apparatus consisted of an impact assembly and its guiding cables, a velocity measuring system, a level

*Additional information on Pneumacel and polyurethane foam can be found in Appendix A.

QAW/MC/72-3

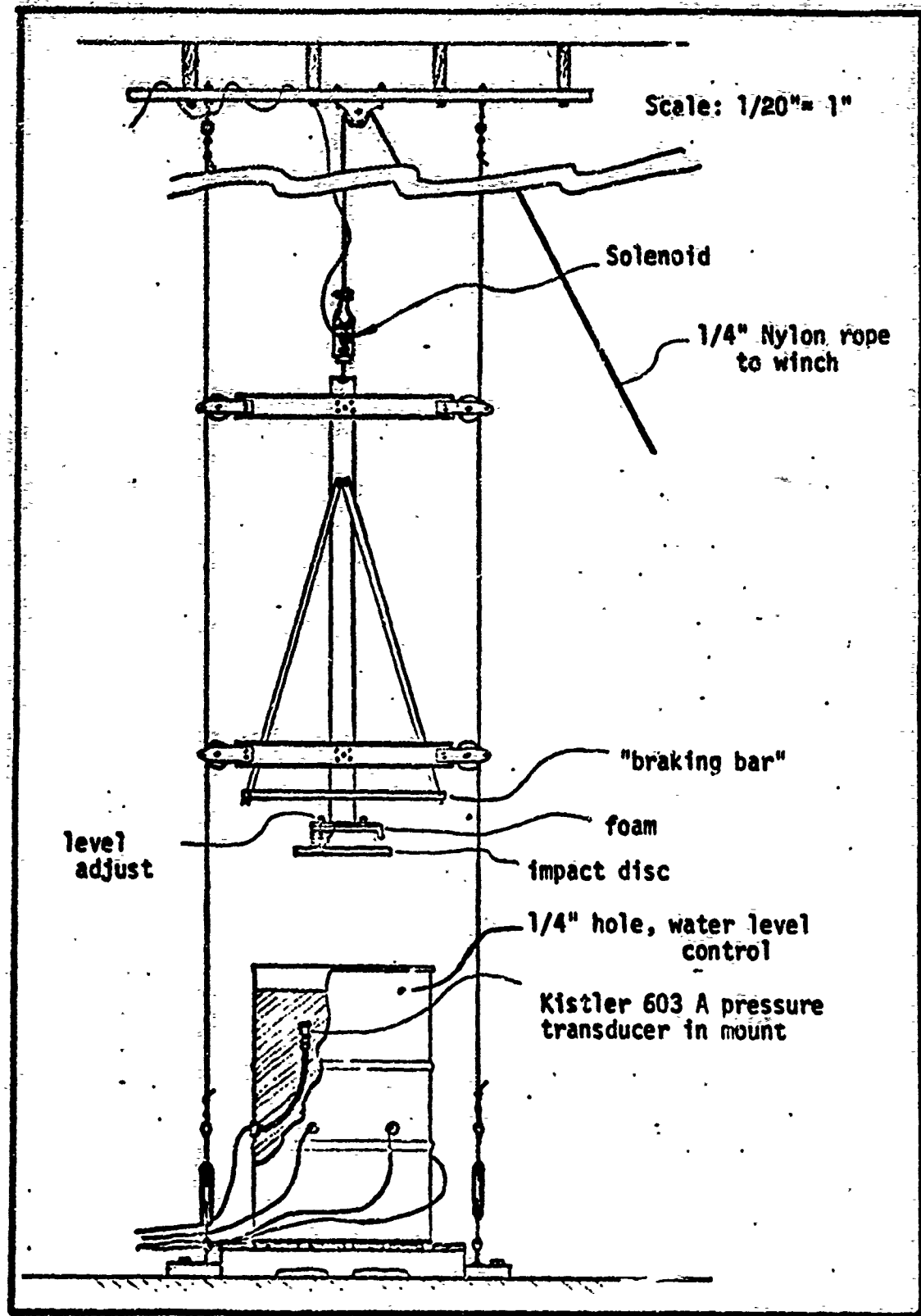
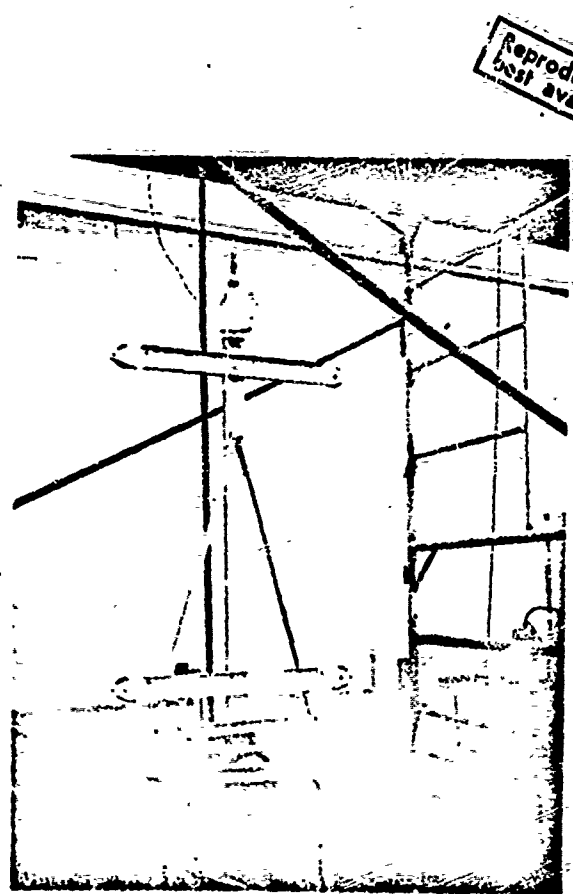


Figure 1
Experiment I, General Apparatus Layout

measuring system, and the target tank as shown in Figure 1. The impact assembly (Figure 2) consisted of an impact disc, a guiding assembly, and a release mechanism. The impact disc was a 2.54 cm thick flat plate of 2024 aluminum turned on a lathe to an outside diameter of 30 cm. The impact disc was bonded to a 2 in. thick 7 7/8 in. diameter disc of 2024 aluminum. Three holes were drilled and tapped for 10x32 screws, 120° apart and 7/16 in. from the edge of the second disc. The two discs were attached to the bottom of the



Reproduced from
best available copy.

Figure 2
Impact Assembly

guiding assembly by three 10x32 bolts passing through a $\frac{1}{2}$ in. thick aluminum plate and a 2 in. thick block of polyurethane foam (2 in. thick before compression and approximately $\frac{1}{2}$ in. thick after compression). The three attachment bolts provided a simple method for leveling the disc.

The main vertical and horizontal members of the guiding assembly were constructed of 3x1 in. steel channel. At the ends of each horizontal arm were 3 in. outside diameter cable pulleys. The pulleys were mounted in brackets that allowed small adjustments to be made in the horizontal plane. Below the lower horizontal arm was a "braking" bar of $1\frac{1}{2} \times 1\frac{1}{8}$ in. 2024 aluminum channel braced at the ends by 1 in. square 2024-T3 aluminum tubing. This bottom bar was installed to stop the assembly after it impacted the target to prevent damage to the gages mounted below. The bar could be quickly changed if it was damaged. The impact assembly was designed and constructed so that its center of gravity lay along a line down the center of the outside of the vertical shaft. The assembly was hung by its attachment point at the top, and checked with a plumb line for accuracy of vertical alignment and the pulleys were adjusted to be in the same vertical plane as the center of gravity. The release mechanism was a solenoid attached to a $\frac{1}{4}$ in. nylon rope with electrical wires running to a toggle switch and a 24 volt battery. Except during planned drops of the impact assembly, a safety mechanism consisting of two "C" shaped aluminum plates was clamped over the solenoid to prevent an accidental drop of the impact assembly. A winch raised and

lowered the 44.5 pound impact assembly.

Two 3/32 in. steel cables were attached to a plate fastened to the roof of the building and through turnbuckles were also attached to a plate anchored to the floor. The attachment points in the two plates were drilled at the same time and the alignment of the eyebolts checked before installation. The bottom plate was positioned below the upper plate by using plumb lines in the upper two eyebolts. After the cables were installed and made taut, their alignment was again checked in two planes with a plumb line. A pulley was attached to the top plate so that the nylon rope to the release mechanism was over the center of gravity line of the impact assembly, and this alignment was checked with a plumb line. Bolts were installed through the pulley brackets to prevent the pulleys from jumping off the cables.

A velocity measuring assembly consisting of five bronze spring brushes, 10 cm apart, was located along the fall path of the impact assembly. The brushes were attached to Plexiglas holders which could be adjusted individually by set screws. The assembly was mounted in such a way that the bottom brush would make contact when the impact plate was 2 cm from the surface of the target. The assembly did not touch the target drum, so no motion could be transmitted to the target before impact. As the impact assembly fell, a copper tab on the lower arm of the guiding assembly contacted the brushes, closing a circuit powered by two 1.4 volt batteries. The electrical pulses generated by the batteries were carried by a coaxial cable to the tape recorder located

in the instrument area.

About 2 in. above the surface of the water was a device designed to measure the attitude of the free falling plate before it hit the surface of the target. The device consisted of a $\frac{1}{2}$ in. thick Plexiglas ring with three bronze spring brushes mounted 120° apart. The hole in the center of the ring allowed 1 3/8 in. clearance from the outer edge of the impact disc. Three holes were drilled in the ring and tapped for $\frac{1}{4} \times 20$ set screws. The set screws extended through the ring supporting it by resting on three small pieces of aluminum angle attached to the inside of the target drum just above the surface of the water. The three brushes were mounted in line with the set screws and extended radially inward into the path of the falling impact disc. When the disc touched each contact it closed a circuit with two 1.4 volt batteries sending an electrical pulse through separate coaxial cables to the tape recorder.

The material to be impacted was contained in an open 55 gallon steel drum. The drum was placed on a wooden pallet which straddled the bottom cable attachment plate so that cable motion and vibration could not be transmitted to the target material. One $\frac{1}{4}$ in. hole was drilled 3 in. below the top of the drum to control the level of the water in the drum. Four 9/16 in. holes were drilled 17 3/4 in. below the water level and fitted with 3/8 in. bulkhead fittings and Teflon seals. Flare fittings and 3/8 in. copper tubing were used to mount four Kistler 603-A pressure transducers in the drum and to protect the transducer wiring from the water.

The transducers were positioned roughly in a 7 in. diameter circle and were located 7.5 cm, 10 cm, 15 cm, and 20 cm below the surface of the water (Figure 3). Gages 1 and 4 were about twice as far apart as the other gages to prevent gage 4 from being in an area influenced by gage 1.

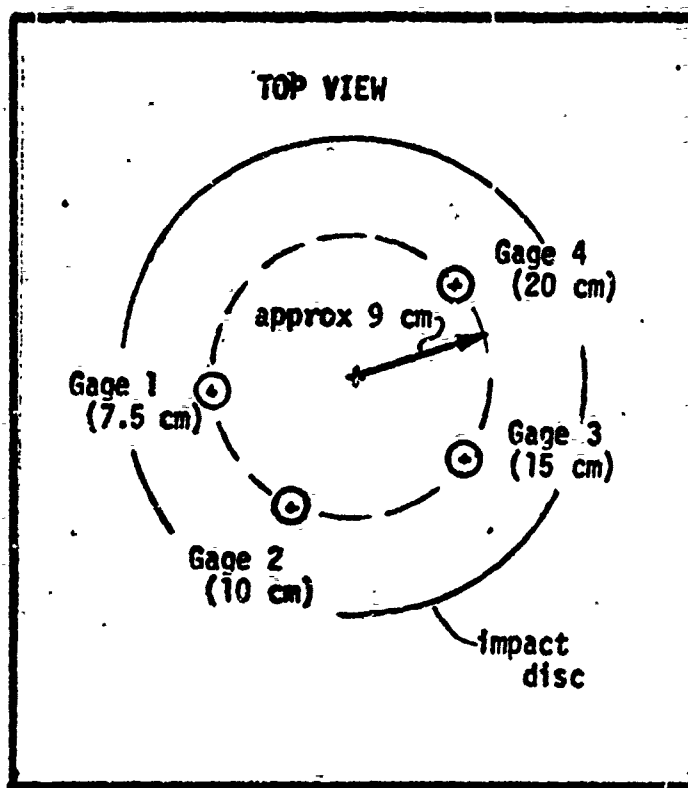


Figure 3
Experiment I. Gage Location

Experiment II. The second part of the experiment was conducted in the Air Force Materials Laboratory Low Velocity Gun Range which is operated by the University of Dayton Research Institute. In this experiment $\frac{1}{2}$ in. steel balls were fired into the same target materials used in the first experiment and pressures were measured at three points. The

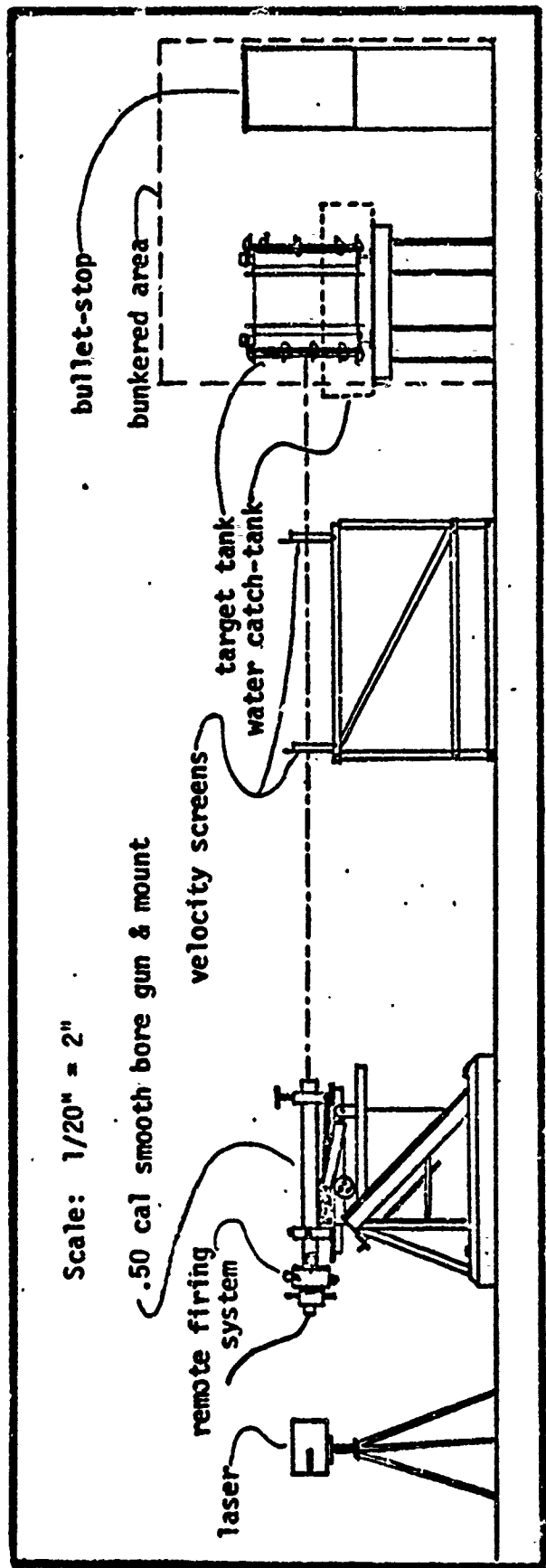


Figure 4
Experiment II General Apparatus Layout

projectiles used were standard $\frac{1}{2}$ in. steel ball bearings. All bearings were .4995 in. in diameter and weighed 128.5 grains. Figure 4 shows the general layout of the principal components of the test apparatus: (1) the aiming laser, (2) the gun mount, (3) the velocity measuring systems, and (4) the target. The beam of a small laser mounted behind the gun was aimed down the bore of the gun so that the impact point could be accurately predicted. The gun used in the experiment was a smooth bore .50 caliber Mann test barrel attached to a Frankford mount. The test barrel was $43\frac{1}{2}$ in. long and the actual bore was 0.502 in. The rear of the barrel was threaded to receive various chambers, and a .30 caliber chamber was used in all tests in this experiment. A screw type breech was attached to the chamber and a remotely controlled solenoid fired the gun.

Between the muzzle of the gun and the target tank were two velocity screens, exactly four feet apart. The screens were connected to the instrumentation and measured elapsed time between successive projectile impacts.

The target was a rectangular tank measuring $23\frac{1}{2}$ in. high, $29\frac{1}{2}$ in wide, and 24 in. deep. The top, bottom, and sides were $\frac{1}{4}$ in. steel plates, reinforced by four bands of 2 in. angle iron. The front and back plates were removable and were made of 0.125 in. 2024 aluminum. Each plate was held to the tank by a frame of welded $1\frac{1}{2}$ in. angle iron and 14 $1\frac{1}{2}$ in. "C" clamps. A small bead of putty was used as a seal between the plates and the tank. A 4 in. diameter hole was cut in the center of the front plate and a $1\frac{1}{2}$ in.

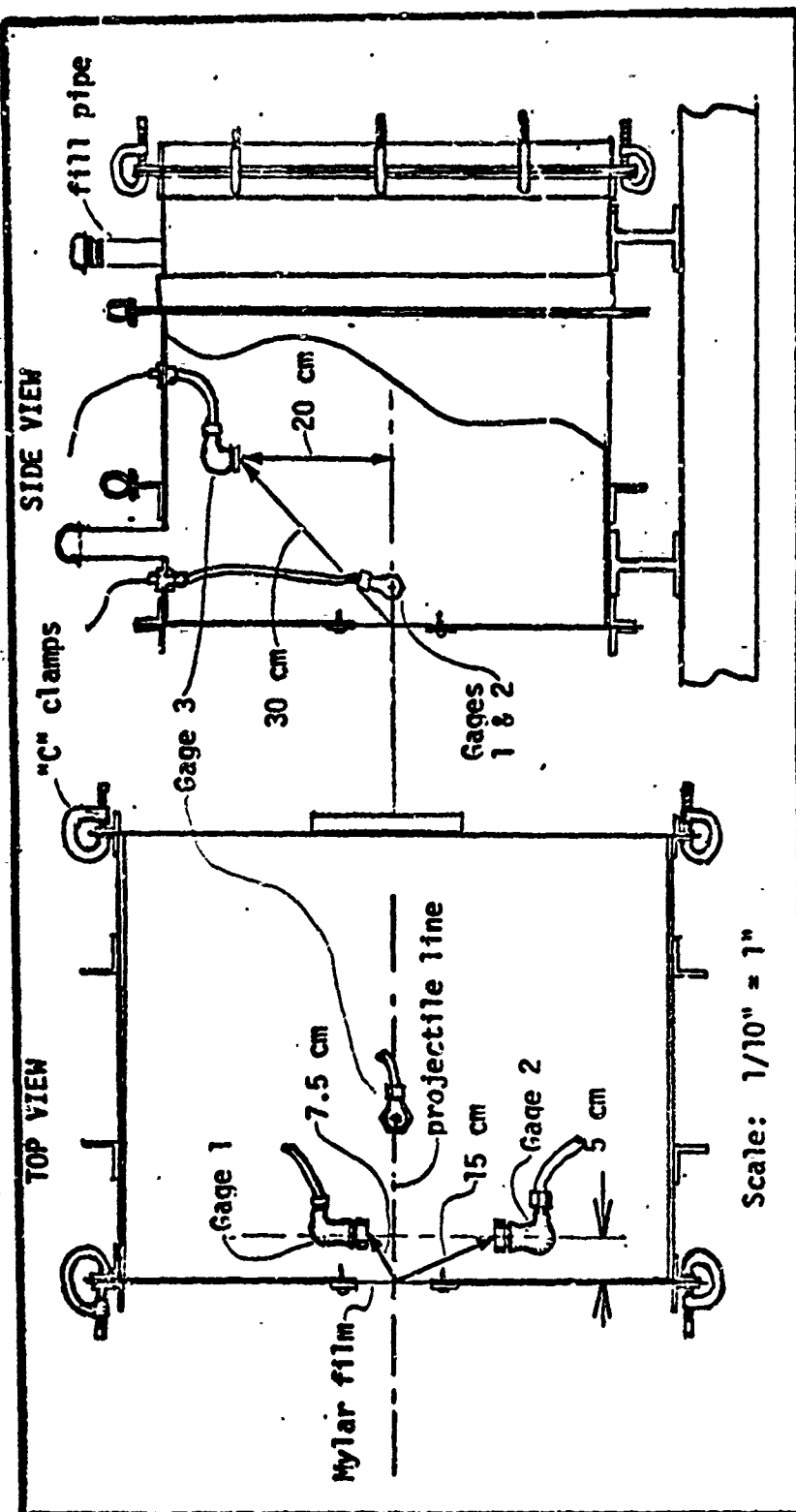


Figure 5
Experiment II Target and Gage Location

wide collar made to hold a .0005 in. Mylar sheet over the opening. Eight sheet metal screws attached the collar to the plate. An 8 in. square piece of 1 in. thick aluminum was fastened to the center of the back plate to prevent the projectiles from penetrating the back plate.

Three Kistler 603-A pressure transducers were mounted in the tank by 3/8 in. copper tubing and various flare fittings. Two gages were positioned at opposite sides of the projectile path, 5 cm from the front plate, and 7.5 cm and 15 cm respectively from the impact point (Figure 5). The third gage was located 2 cm above the path of the projectile and 30 cm from the point of impact. This arrangement was chosen to measure the attenuation of the pressure pulses, and gage 3 was also able to record the pressure field generated by the passing projectile. A catch tank of plastic sheets attached to a wooden frame was constructed around the target tank to catch the water spilled after the projectile ruptured the Mylar film.

Instrumentation

Kistler 603-A quartz transducers with model 105H connector adapters connected to Kistler 504-A charge amplifiers were used to measure the pressure in both experiments. All transducers were mounted in a locally produced aluminum adapter which is used with Kistler gages.

All data were recorded on a Sangamo Model 3562 portable recorder/reproducer. All recording was done in the FM mode at 60 ips, and playback was done at both 60 ips and

1 7/8 ips. For the first experiment, nine channels of data were recorded: four for pressure, one for the reference signal, one for velocity data, and three for checking the attitude (level) of the impact disc. In the second experiment, only four channels (three for pressure and one for a reference signal) were used. The reference was a 1.0 KHz, 1 volt signal generated by a Hewlett Packard Model 220CD Wide Range Oscillator. The frequency was checked by a Hewlett-Packard Model 521CR Electric Counter, and the voltage was calibrated by a Simpson Electric Company Multimeter. An Eldorado Counter, Model 1410, was used with the velocity screens in the second experiment. A Honeywell Model 1508 Visicorder Oscillograph and a Tektronix Type 549 Storage Oscilloscope with a type 53/54C dual trace plug-in unit and Tektronix C-19 Oscilloscope Camera using Polaroid Type 47 film were used to interpret the data recorded on the tape.

III. Experimental Procedures

The instrumentation was calibrated as stated in Appendix B and in accordance with the appropriate technical manuals.

Experiment I

A total of 18 drops of the impact assembly were made in the first experiment. Twelve of these constituted successful data runs. The first four were made for operational checks of the entire system and calibration of the equipment. The results of run 10 were discarded because of uncertainty about the water level in the drum, and run 11 was a repeat of that run. The last run was a check of the calibration and functioning of the transducers. The first two and the last run were made with all four transducers at the same depth.

For the recorded runs, four drops were made against each target material, with nominal drop heights of 0.5 m, 1.0 m, 1.5 m, and 2 m. The heights of the drops were not exactly the same each time because small adjustments could not be made with the winch that lifted the impact assembly.

The procedures for each drop were as follows:

1. The instrumentation was turned on to warm up.
2. The water level in the drum was made a little too high and allowed to drain through the level control hole to attain the proper level.
3. The depth of the gages was checked.*

*Depth of gage check was difficult with the foams in the drum; therefore it was necessary to check the depth of the gages before installation of foam and after removal. Depth did not vary over 2 mm in any case.

4. The impact disc was leveled by adjusting the securing bolts until the dry disc, lowered very slowly, touched the water in a level condition.*
5. The level-check ring was adjusted by connecting the circuits two at a time to a dual trace oscilloscope and adjusting the set screws until both brushes touched simultaneously when the disc was lowered very slowly.
6. The velocity measuring brushes were adjusted to 2 cm, 12 cm, 22 cm, 32 cm, and 42 cm above the surface.
7. The impact assembly was raised to approximately $\frac{1}{2}$ in. below the desired drop height.
8. The hook-up of the instrument circuits to the tape recorder was checked.
9. The reference signal was adjusted to 1 KHz and 1 volt.
10. The thermostats in the building were turned down to turn off the heater fans that vibrated the ceiling and guiding cables.
11. The necessary information was recorded: drop height, number, target material, tape recorder counter setting, and circuit to channel hook-up.
12. The solenoid was connected to the battery and the toggle switch was set to "Hold".
13. The impact assembly was lifted approximately $\frac{1}{2}$ in. to engage the solenoid.
14. The solenoid safety was removed.
15. The ground button of each Kistler charge amplifier was pressed to dissipate any accumulated charge..
16. The tape recorder was set to "START-RECORD".
17. After the tape speed had stabilized, the toggle switch was moved to "DROP", thus releasing the impact assembly.

*Leveling the disc was difficult with the foams in the drum unless the water level control hole was plugged, and the water level was raised slightly during leveling. The water was then lowered to the proper level.

18. The tape recorder was set to "STOP".
19. The battery was disconnected from the solenoid.
20. The data for that run was checked on the oscilloscope to be sure that all elements of the experiment functioned.
21. The impact assembly was checked and the "braking" bar was replaced if necessary.

Pneumacel tended to float and had to be held down in the drum with safety wires fastened between boards wedged into the bottom of the drum and pieces of heavier wire laid on top of the Pneumacel. To prevent the buoyancy from appreciably compressing the Pneumacel mat, the material was placed only in the top 14 in. of the drum, and the material was secured by the safety wire at the surface and also 7 in. below the surface. The wires securing the Pneumacel were to the outside of the area impacted except for one in the center.

Experiment II

A total of 22 shots were fired in the second experiment. The first two shots were fired to obtain a curve of powder charge versus projectile velocity, and were not fired into the test target. The next 10 shots were fired into the test target: four into water, three into the water-foam mixture, and three into water-Pneumacel. One shot at each of a high, medium, and low velocity was fired into each target mixture. An analysis of the data made after the first 10 shots had been fired showed that gage 2 (15 cm) was intermittently failing. Investigation of the circuits revealed that the cable shield was shorting under impact loads where it connected to the transducer adapter. The faulty cable was replaced

and the entire sequence of ten shot was repeated.

Generally, projectiles are launched from smooth bore guns with sabots. However, in this case the small clearance between the bore and the projectile made this impractical. Instead a muzzle loaded ball and patch technique was used. A cross shaped patch consisting of two $1\frac{1}{2}$ in. long, $\frac{1}{2}$ in. wide, and .0035 in. thick pieces of Teflon tape was placed over the muzzle and the ball was forced into the bore. Good control over velocity and impact point was achieved.

The procedures for each shot were as follows:

1. The instrumentation was turned on to warm up.
2. The gun-target alignment was checked with the laser.
3. The 4 in. hole in the front tank plate was sealed with a Mylar film.
4. The tank was filled with water, and the filler pipes were capped.
5. The velocity screens were set and their circuit checked.
6. The cartridge was loaded with the powder calculated to give the desired projectile velocity.
7. The projectile and Teflon patch were muzzle loaded.
8. The chamber was attached to the gun tube, and the cartridge was loaded.
9. The breech-firing pin assembly was attached to the chamber.
10. The "ground" buttons on the Kistler charge amplifiers were pressed.
11. The remote firing circuit was connected to the gun.
12. The necessary information was recorded: shot number, tape counter setting, and target material.

13. The reference signal was adjusted to 1 KHz, 1 volt.
14. The tape recorder was set to "START-RECORD".
15. After the tape speed stabilized, the gun was fired.
16. The tape recorder was set to "STOP".
17. The projectile velocity was calculated from the velocity screen data and then recorded.
18. The target material was changed if necessary.
19. Shots into water-Pneumacel created a hole approximately 1 in. in diameter in the mat. This hole was filled with loose fibers and pieces of Pneumacel mat to approximate the original target material density.

IV. Results and Discussion

Results.

The results of the twelve successful tests conducted in Experiment I are shown and discussed. The data on the tape recorder were reproduced on Visicorder film for analysis.

Illustrations of the Visicorder films are shown in Figures 6-9. The traces run from right to left and the time reference is from the arrival of the pulse at gage 1. The run number, target material, impact velocity, and maximum pressures (gage) at each gage are shown in Table V in Appendix D.

The data for Experiment II were read first on the Visicorder and then on the storage oscilloscope. Illustrations of the Visicorder film and representative scope photographs are shown in Figures 10-19. The oscilloscope traces run from left to right. The results of all twenty experimental shots are shown. Since some gage 2 readings in the first ten shots are missing, and doubt exists about the accuracy of others, the results and discussion will generally consider only the last ten shots. The values that appear in the tabulated data (Table VI, Appendix D) were read from Polaroid photographs of the storage oscilloscope because amplification of some traces made possible more accurate interpretation. Table VI lists the number of the shot, the target material, and the maximum pressure (gage) recorded at each gage. Listed in Table VI as $P'3$ is the estimated pressure of the initial pulse when it arrived at gage 3. This pressure was read from the gage 3 trace at the time equal to the time the

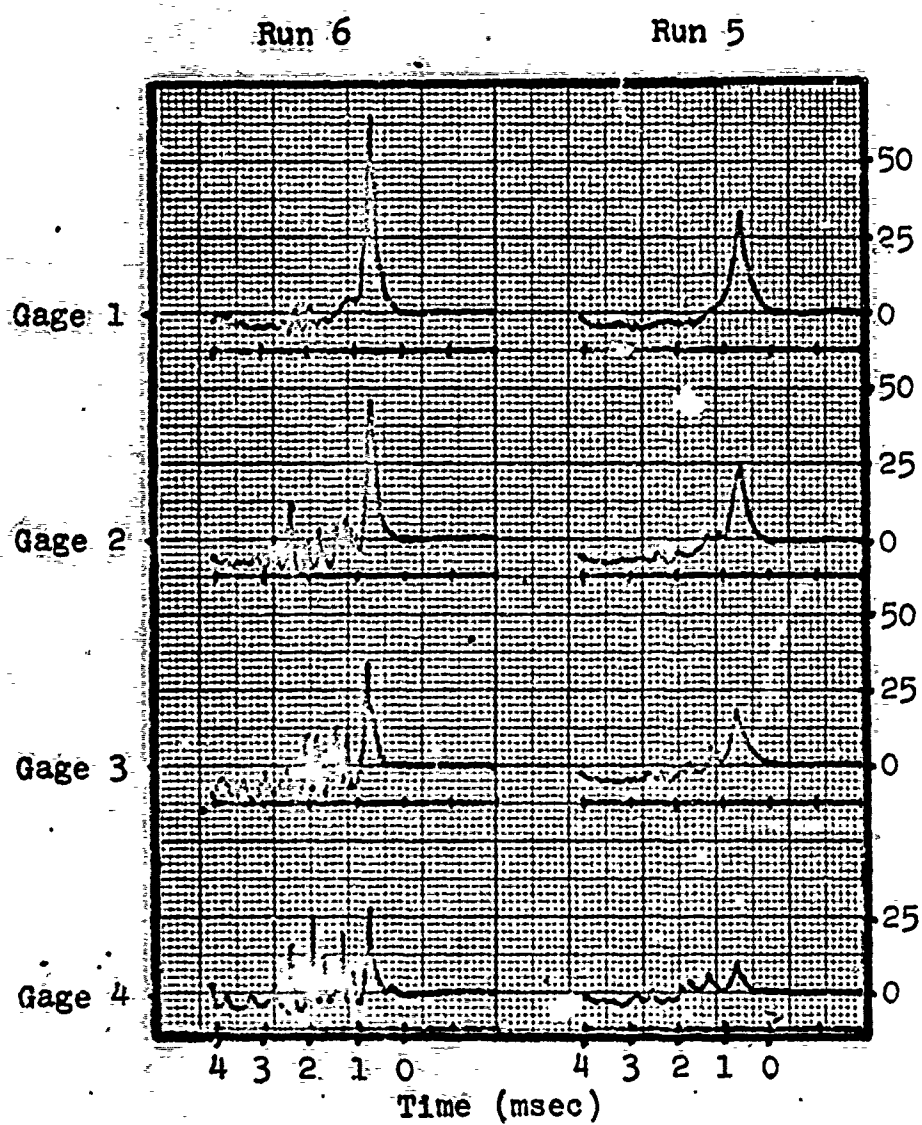


Figure 6

Visicorder Data, Runs 5 and 6, water

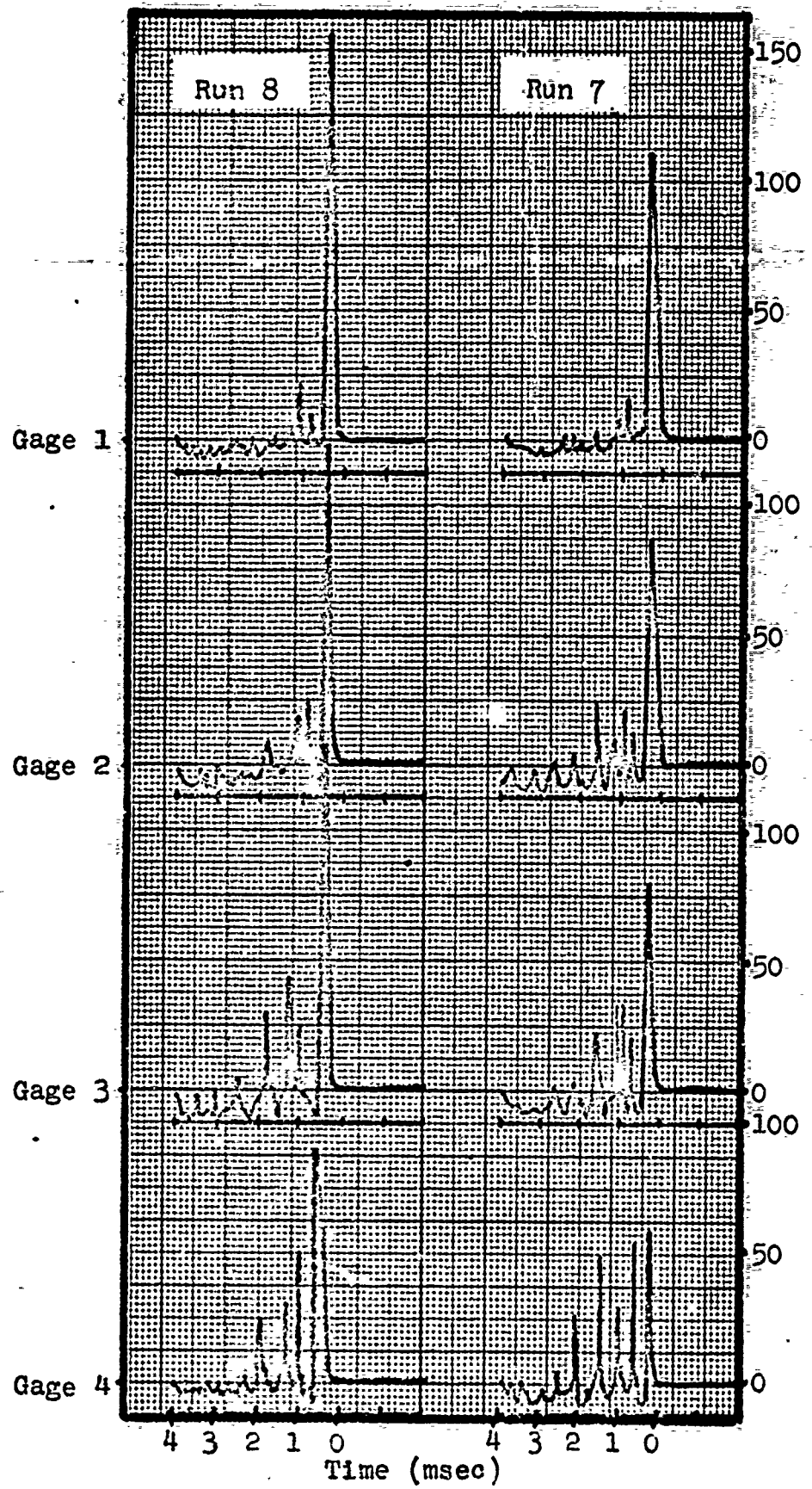


Figure 7, Visicorder Data, Runs 7 and 8, water

GAW/MC/72-3

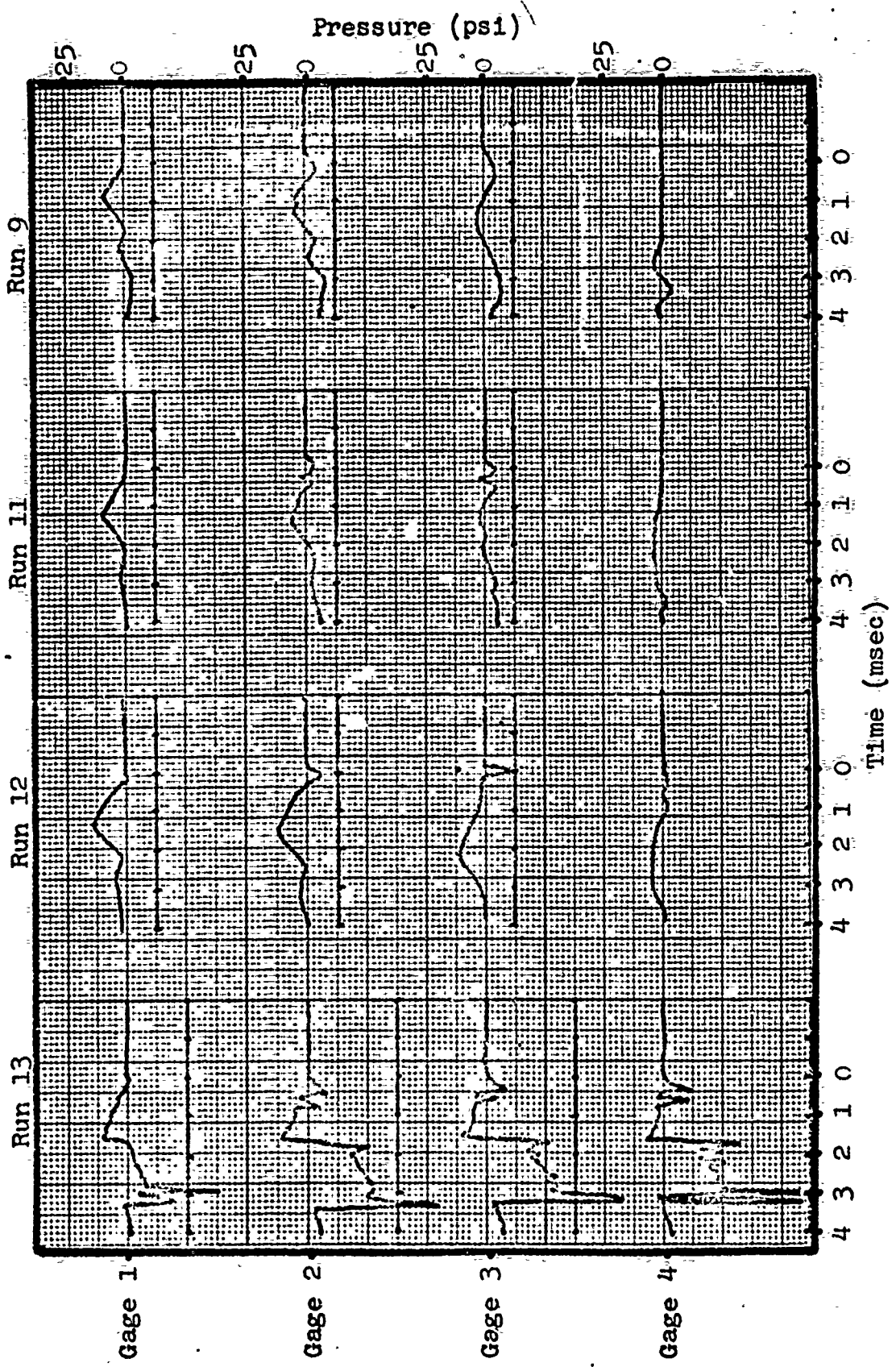


Figure 8, Visicorder Data, Runs 9, 11, 12, and 13, Pneumacel

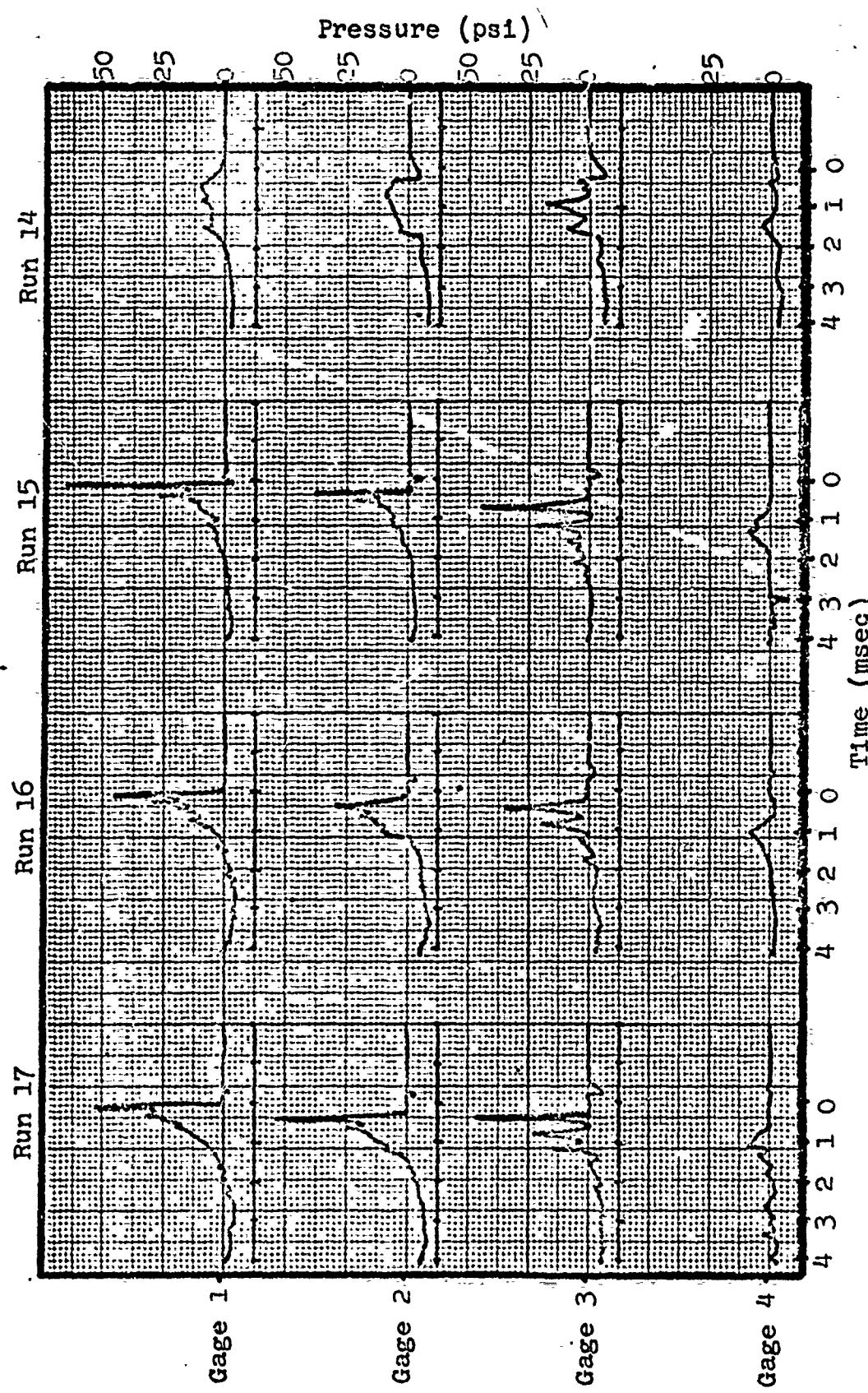


Figure 9, Visicorder Data, Runs 14, 15, 16, and 17, Foam

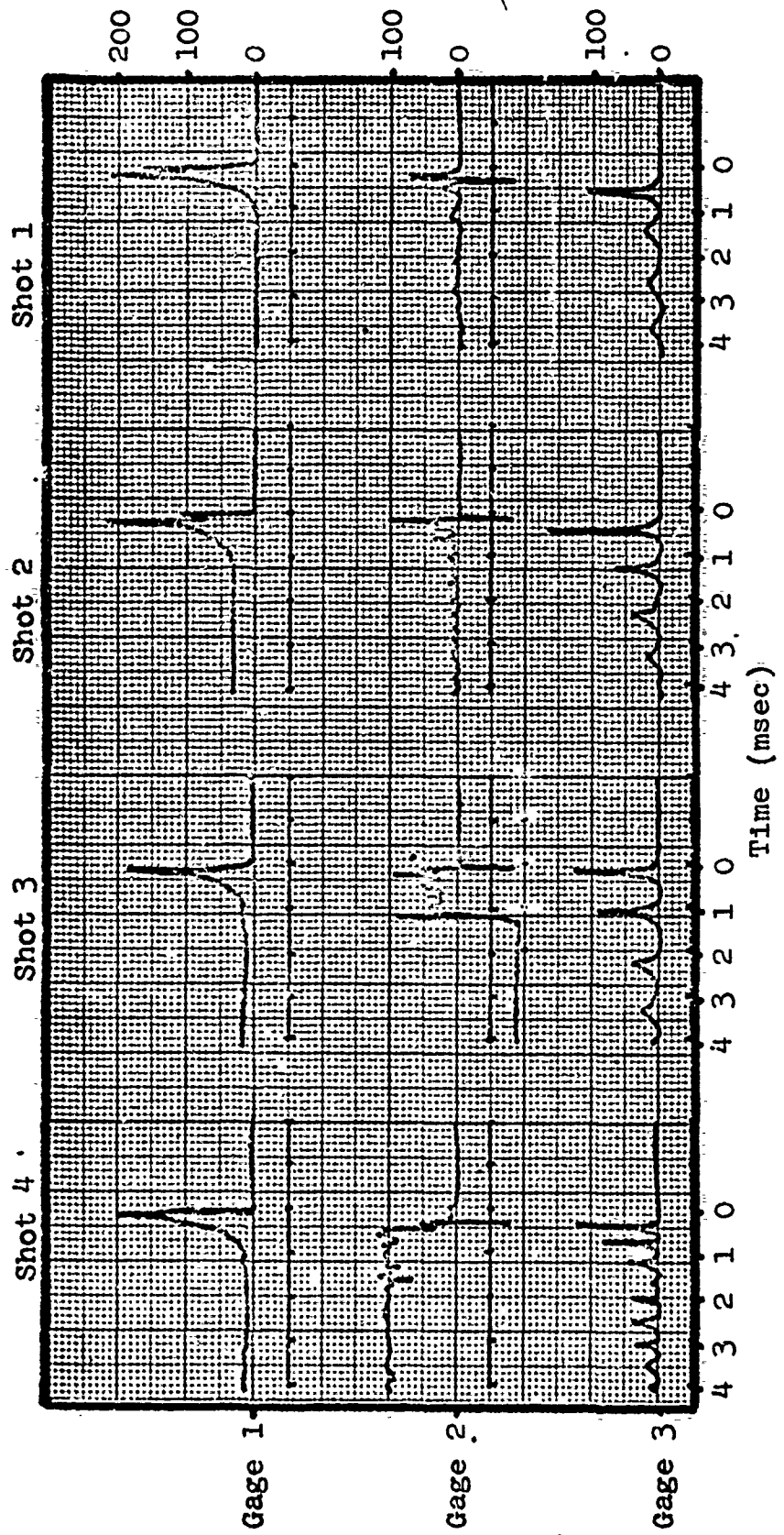


Figure 10, Visicorder Data, Shots 1, 2, 3, and 4, water

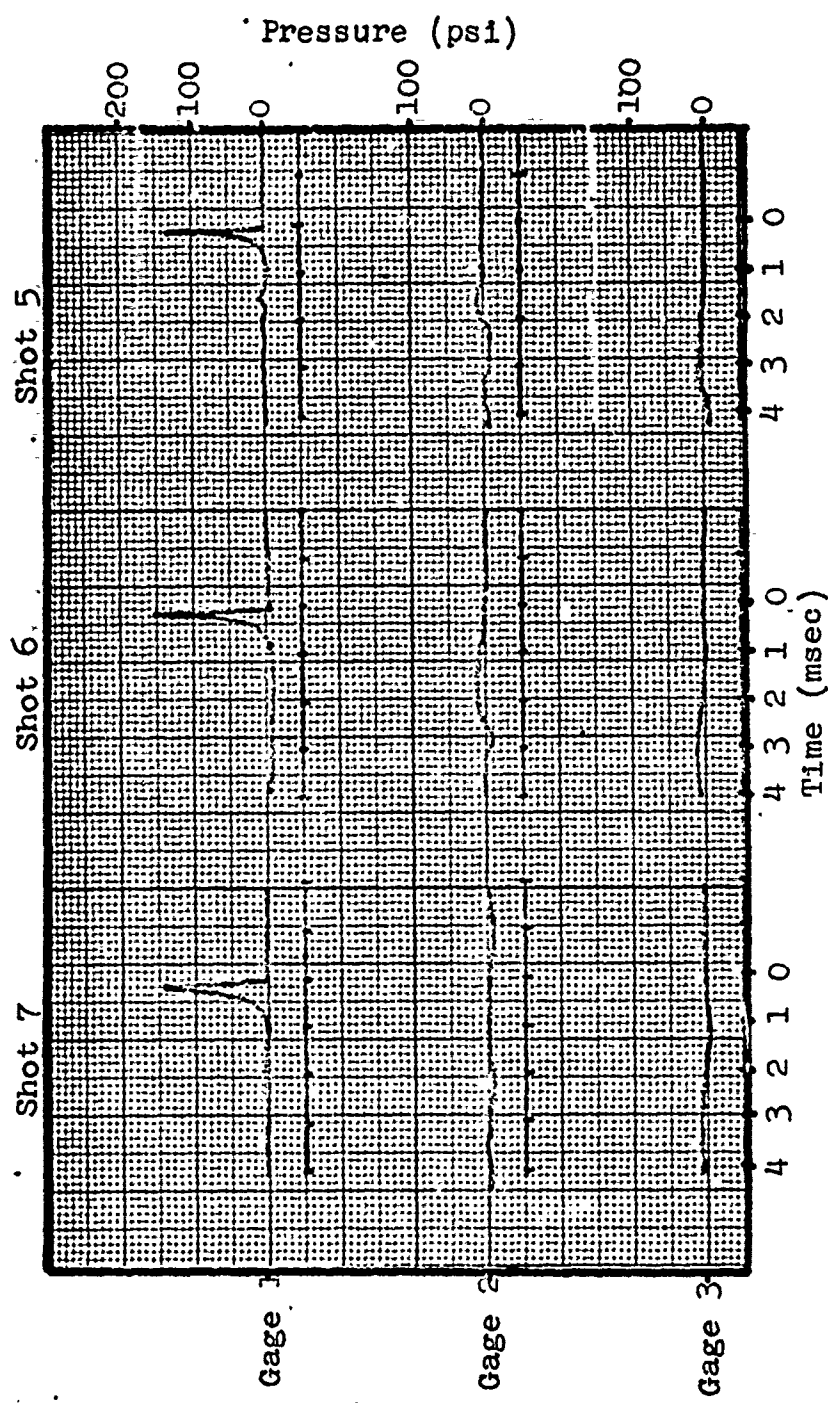


Figure 11, Visicorder Data, Shots 5, 6, and 7, Pneumacel

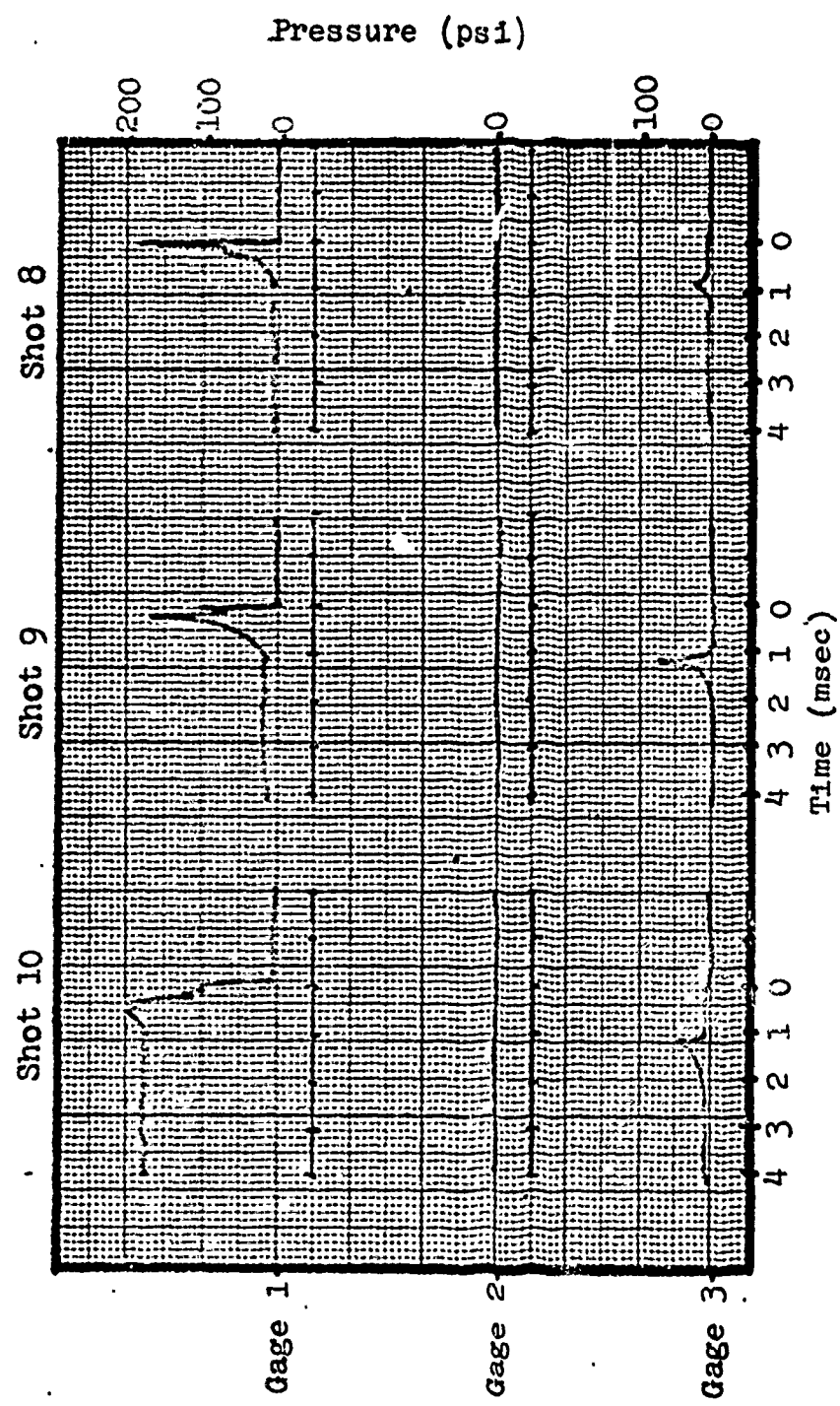


Figure 12, Visicorder Data, Shots 8, 9, and 10, foam

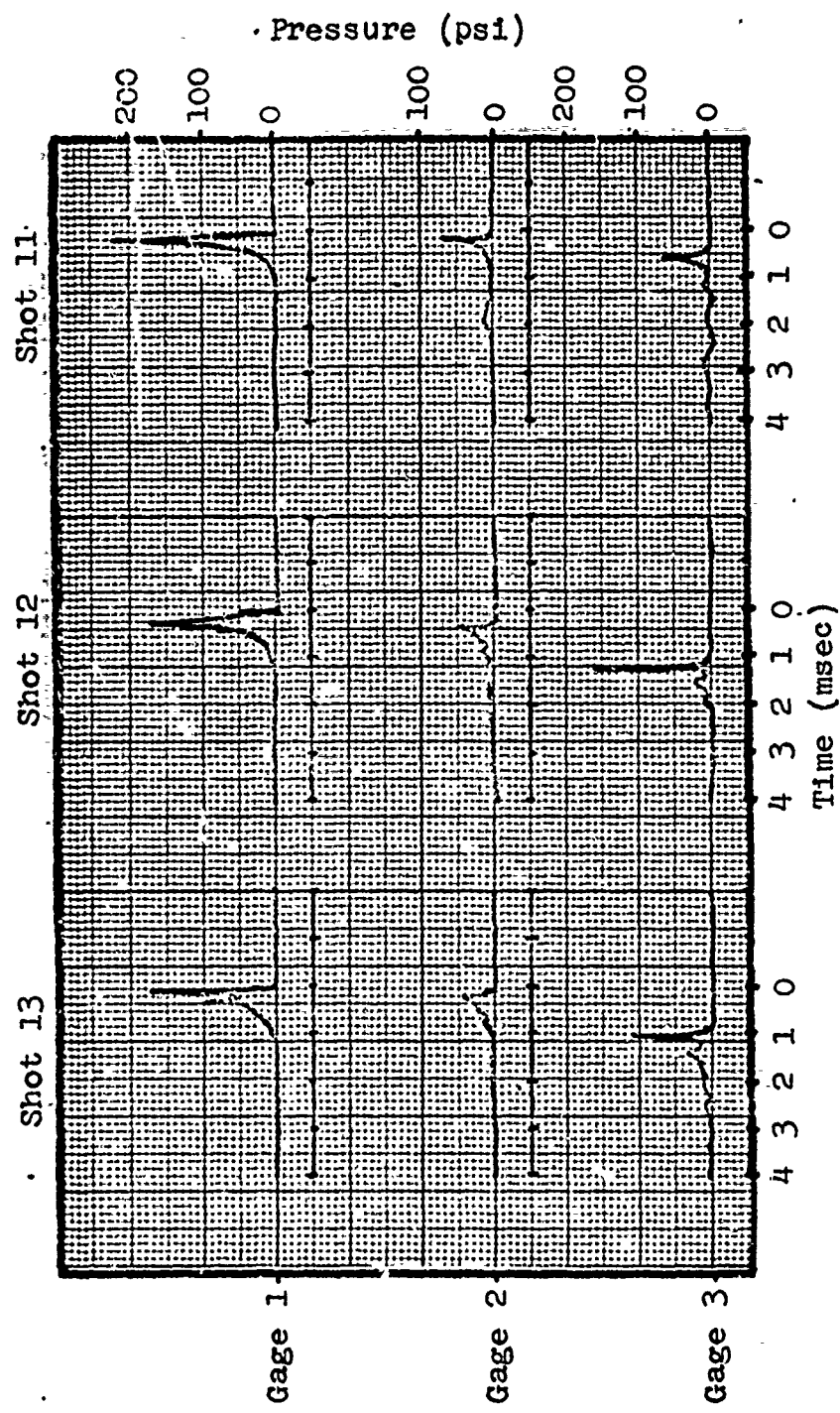


Figure 13, Visicorder Data, Shots 11, 12, and 13, foam

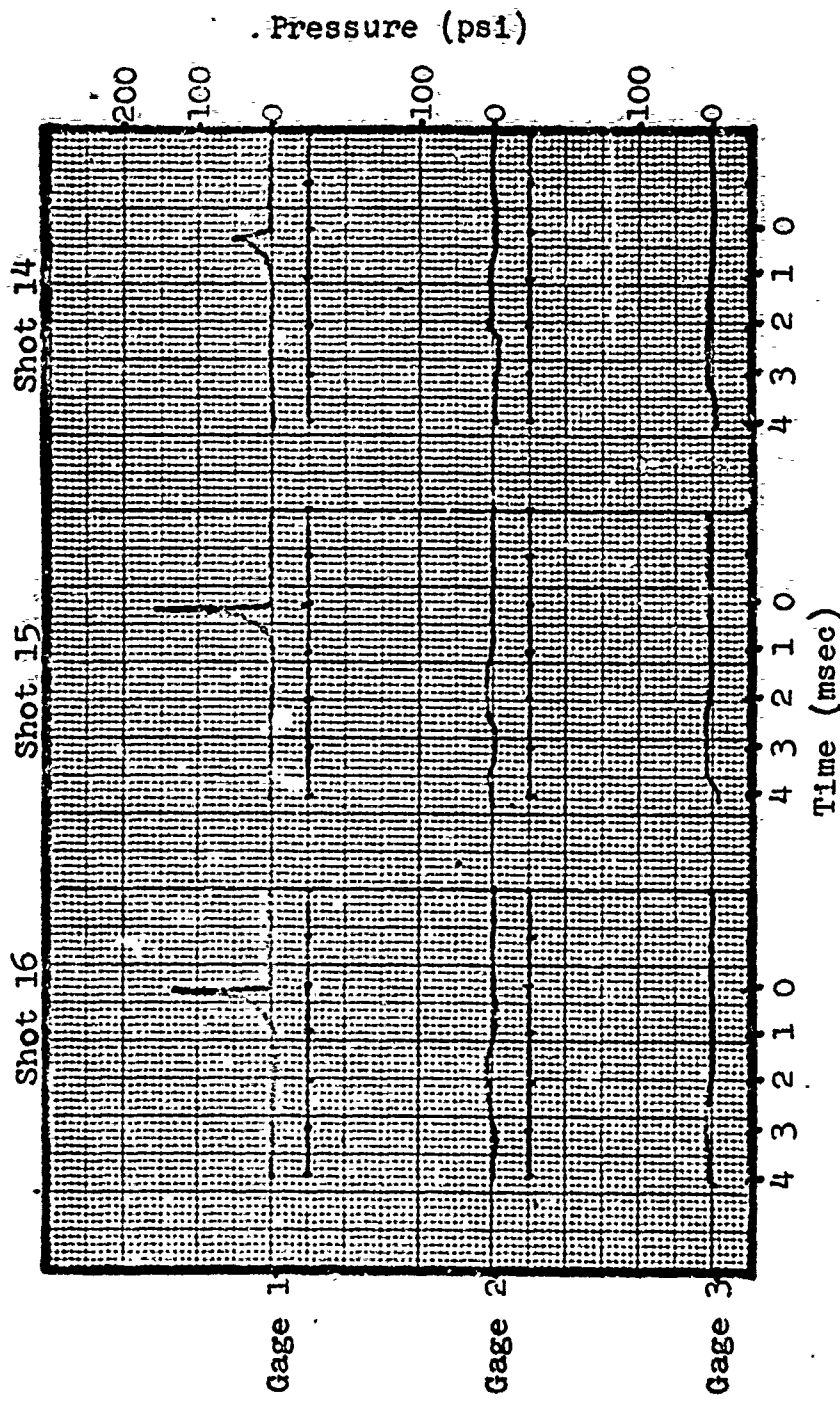


Figure 14, Visicorder Data, Shots 14, 15, and 16, Pneumacel

GAW/MC/72-3

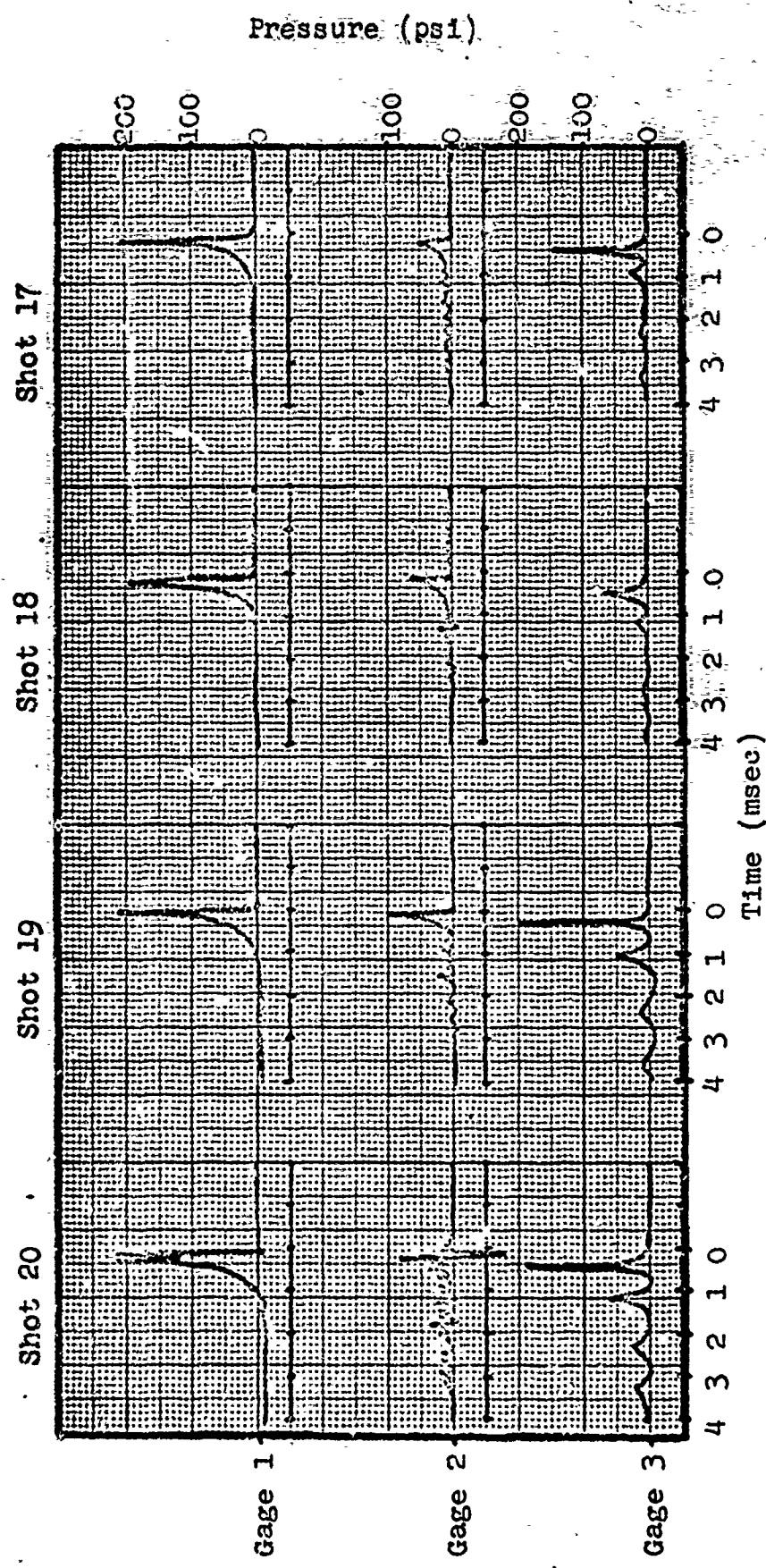
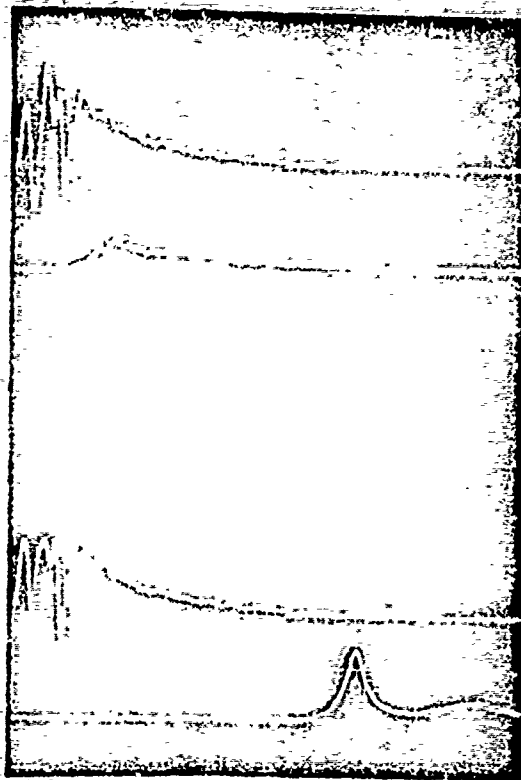


Figure 15, Visicorder Data, Shots 17, 18, 19, and 20, water



Shot 13

Foam

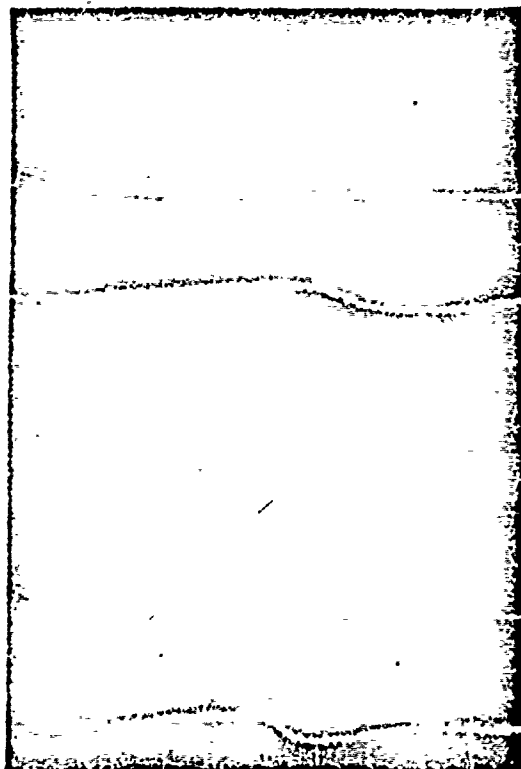
Gages 1 & 2, 1 cm vert
1 volt

1 cm horz
5/32 msec

Gages 1 & 3 same as
above

Figure 16
Scope picture, Shot 13

Reproduced from
best available copy.



Shot 14

Pneumacel

Gage 1 . . . 1 cm vert
1 volt
Gage 2 . . . 1 cm vert
.2 volt
both . . . 1 cm horz
5/16 msec

Gage 1 . . . 1 cm vert
1 volt
Gage 3 . . . 1 cm vert
.2 volt
both . . . 1 cm horz
5/8 msec

Figure 17
Scope picture, Shot 14

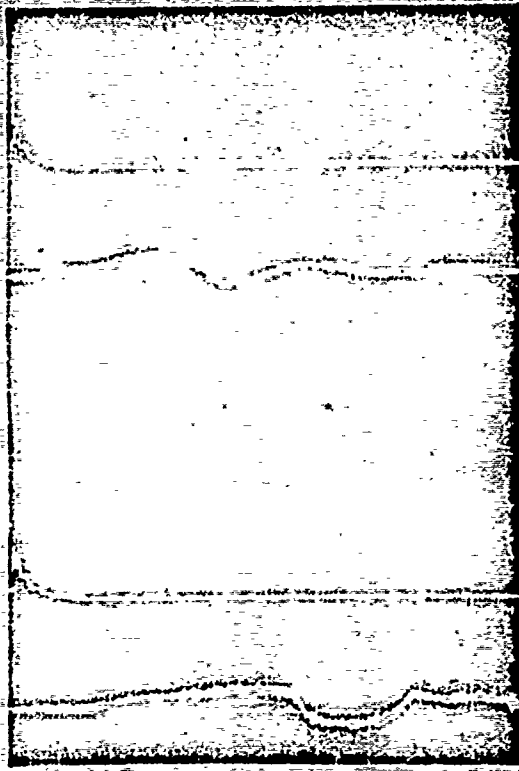


Figure 18
Scope picture, Shot 15

Shot 15

Pneumacel

Gage 1 . . . 1 cm vert
1 volt
Gage 2 . . . 1 cm vert
.2 volt
both . . . 1 cm horz
5/8 msec

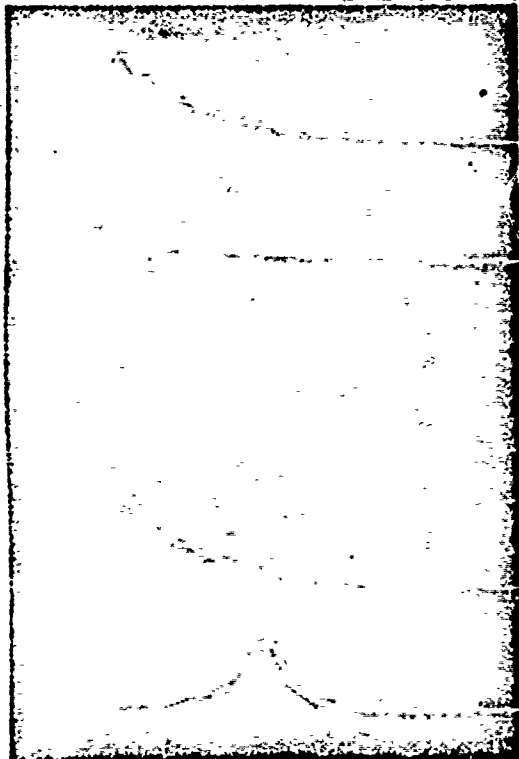


Figure 19
Scope picture, Shot 17

Gage 1 . . . 1 cm vert
1 volt
Gage 3 . . . 1 cm vert
.2 volt
both . . . 1 cm horz
5/8 msec

Reproduced from
best available copy.

Shot 17

Water

Gages 1 & 2, 1 cm vert
1 volt
1 cm horz
1/16 msec

Gages 1 & 3, same as
above

pulse first reached gage 1 plus 3 times the time it took the pulse to travel from gage 1 to gage 2.

Discussion

Experiment I. Before comparing the experimental results of the different runs, a least squares curve fit was applied in an attempt to obtain approximate curves to represent the data. An exponential equation was found to give a satisfactory description of the data. The coefficients and standard errors are shown in Table I.

Table I
Curve Fit Coefficients for $P = P_0 e^{-ax}$
and Standard Error

Run	Drop Height	P_0 (bars)	a (cm^{-1})	S.E. (bars)	P_0 (psi)
5W*	$\frac{1}{2}$	4.78	-0.10111	0.0757	69.21
6W	1	7.16	-0.07066	0.263	103.89
7W	$1\frac{1}{2}$	10.48	-0.04862	0.581	152.02
8W	2	13.60	-0.03610	1.272	197.10
9P	$\frac{1}{2}$	1.87	-0.17123	0.0739	27.16
11P	1	2.61	-0.18841	0.1147	37.81
12F	$1\frac{1}{2}$	1.47	-0.04878	0.1127	21.26
13P	2	1.72	-0.09401	0.1290	25.22
14F	$\frac{1}{2}$	0.941	-0.01668	0.373	13.66
15F	1	8.97	-0.09775	0.947	130.03
16F	$1\frac{1}{2}$	5.32	-0.07862	0.839	77.28
17F	2	6.95	-0.06800	0.876	100.8

*W: water, P: Pneumacel, and F: foam.

Although there is no one attenuation coefficient that describes any material, the average of the coefficients for water and water-foam are nearly equal and one half of the coefficients for water-Pneumacel. The data points and curves are plotted together for each drop height (Figures 20-23). Although the P_0 values determined by the curve fit will be used to represent experimental results in some comparisons to be made, they are not results of the experiment and may be in error to a significant degree. The relationship between the impact velocity and the initial pressures in the different target materials was estimated by plotting these extrapolated P_0 values against the impact velocities in Figure 24. The least squares curve fit of the "data" points shows the pressures in water-foam to be approximately functions of velocity to the 1.5 power, while pressures in water-Pneumacel approach a maximum of approximately 30 psi. This would indicate that the pressures generated by the shock wave phase of hydraulic ram could be significantly reduced by the addition of a gas filled foam, such as Pneumacel.

Fowles (Ref 5) calculated the pressures and depth at which attenuation should begin in "perfect" materials. His calculations predict a step increase in pressure with no attenuation until a rarefaction wave reflected from the upper surface of the impact disc arrives, and then a continuing reduction in pressure occurs. Calculations using the Fowles theory for an aluminum disc impacting targets of water and of the two mixtures whose properties were calculated using simple mixture theories (Ref 10) predict much higher

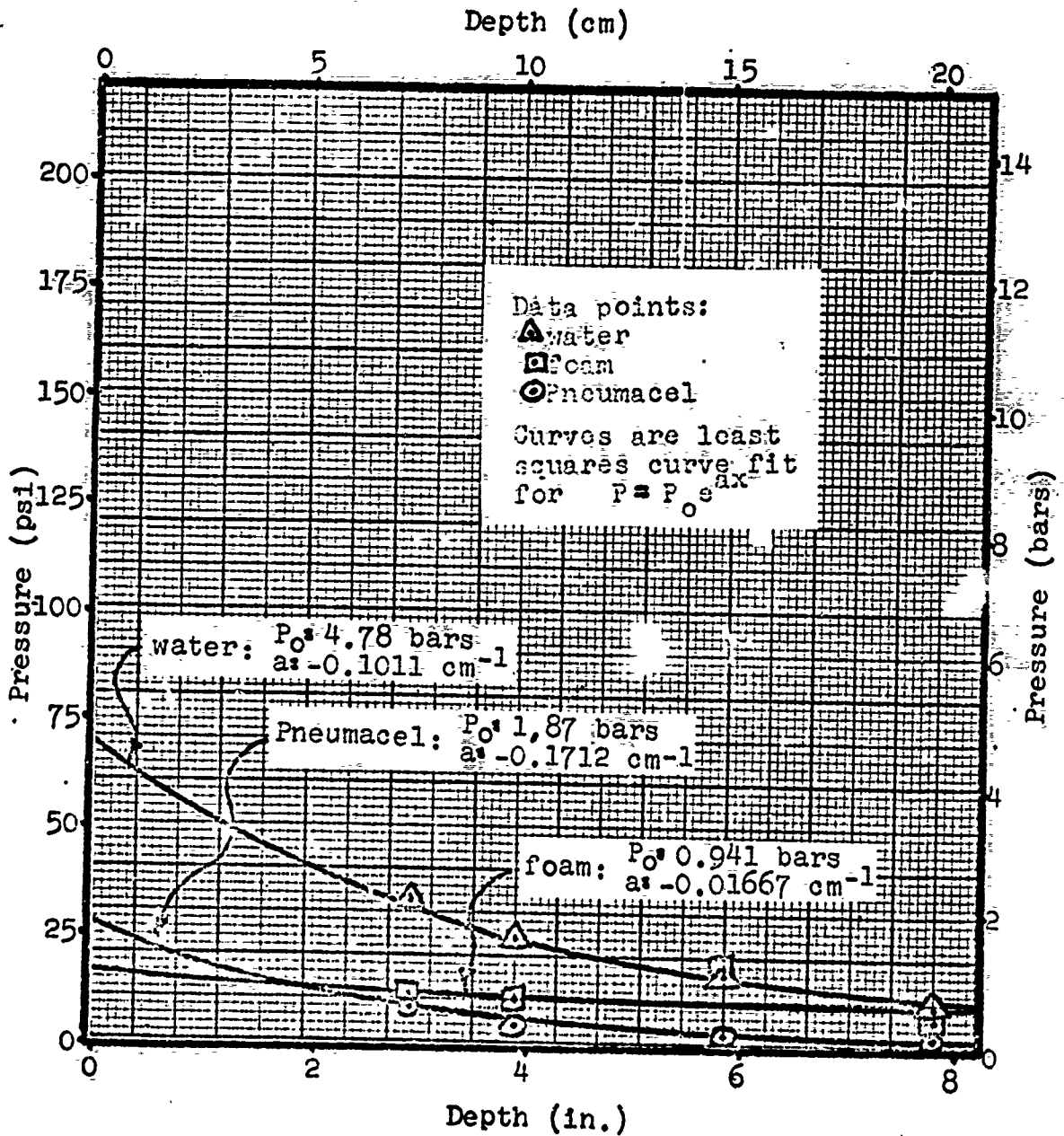


Figure 20

Pressure vs Depth, $\frac{1}{2}$ m Drop

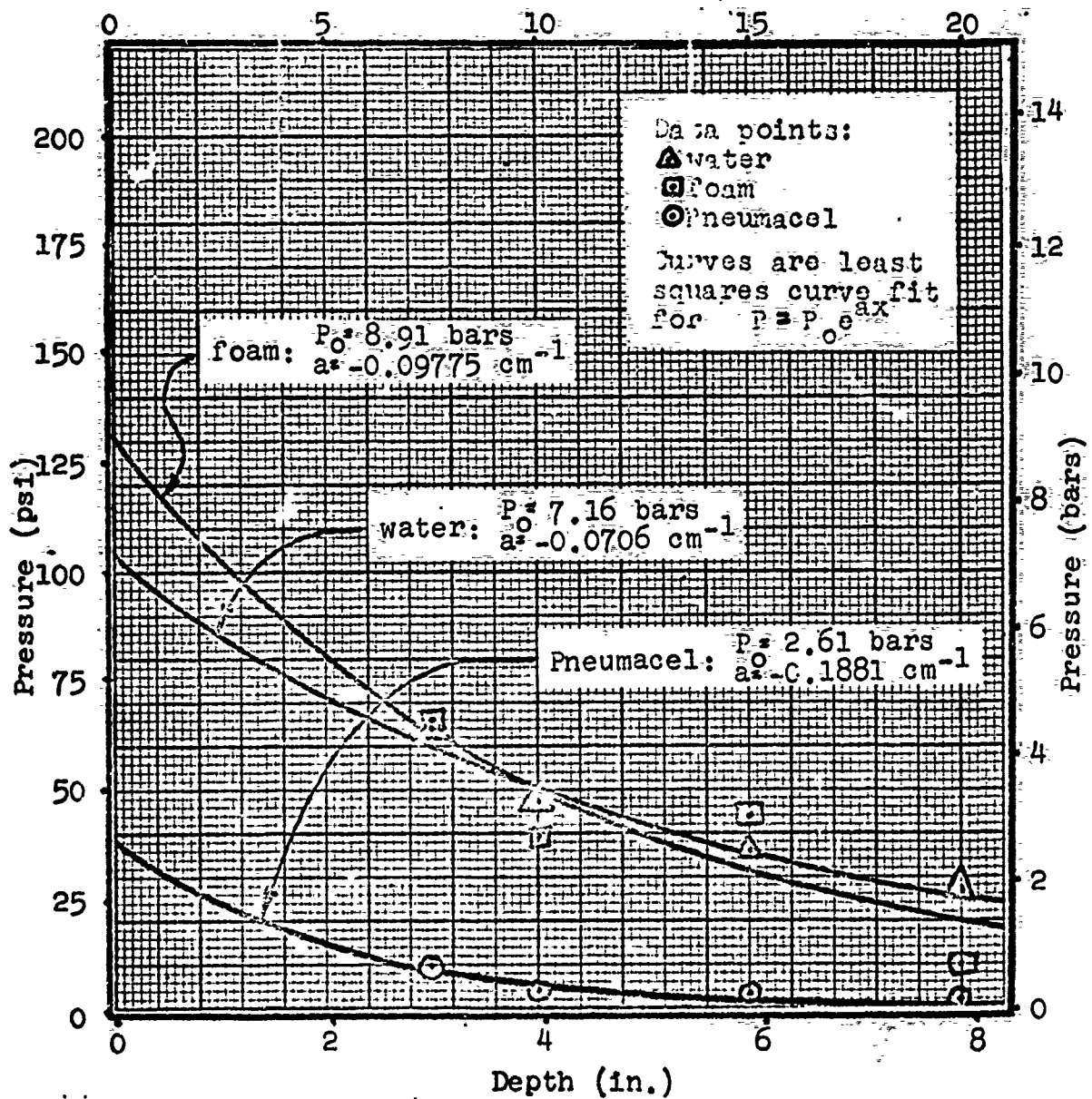


Figure 21

Pressure vs Depth, 1 m Drop

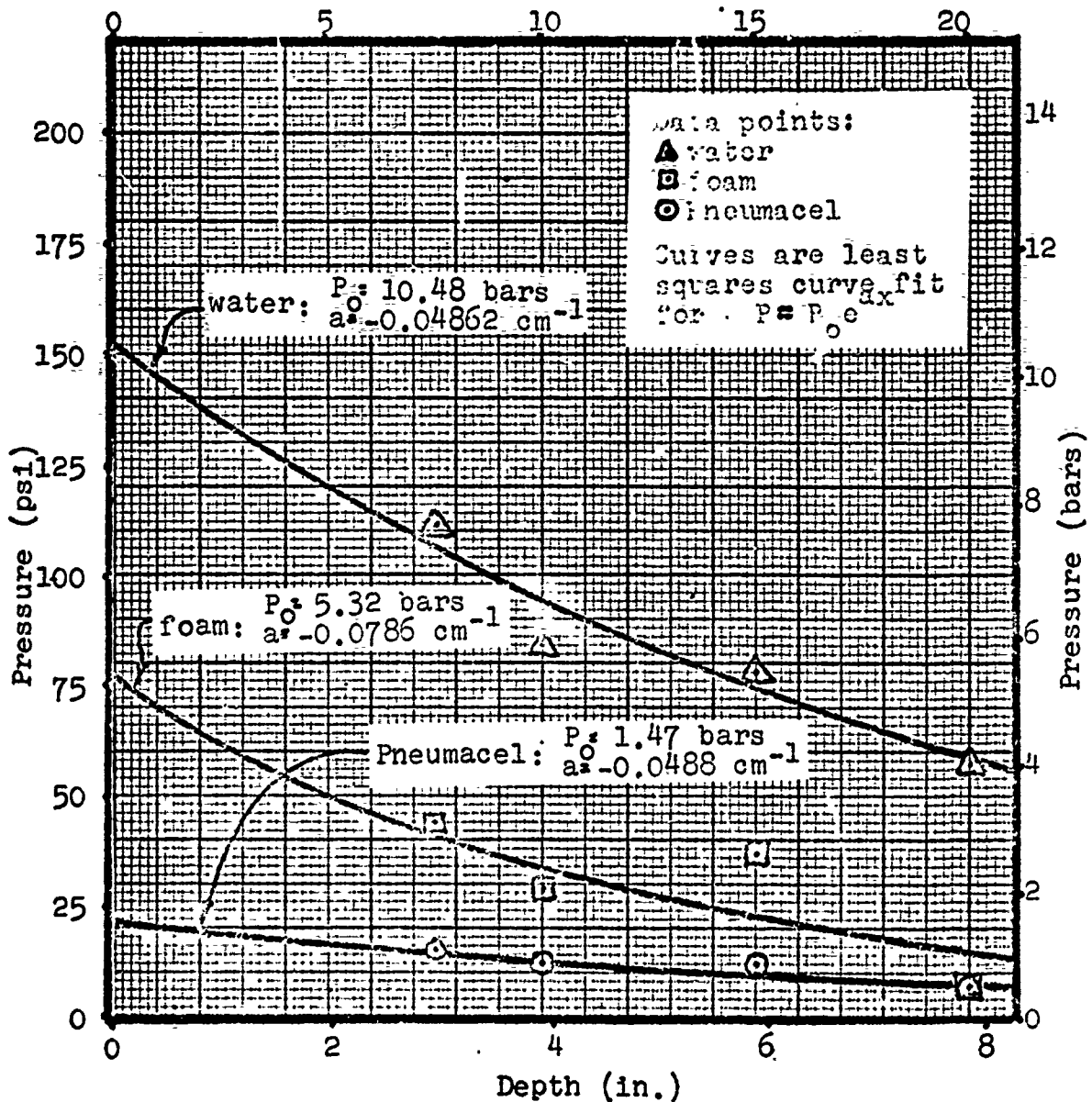


Figure 22

Pressure vs Depth, $1\frac{1}{2}$ m Drop

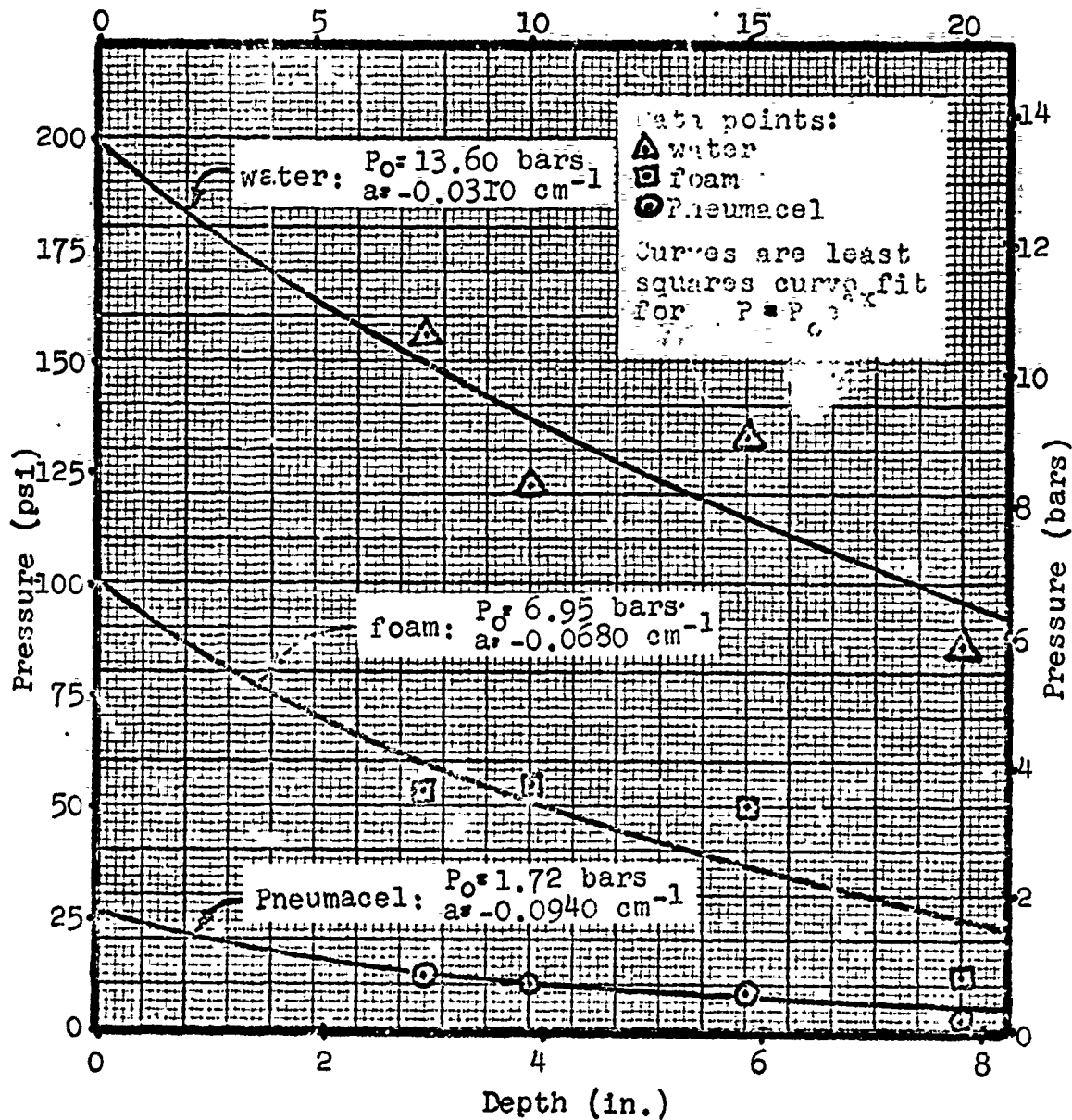


Figure 23

Pressure vs Depth, 2 m Drop

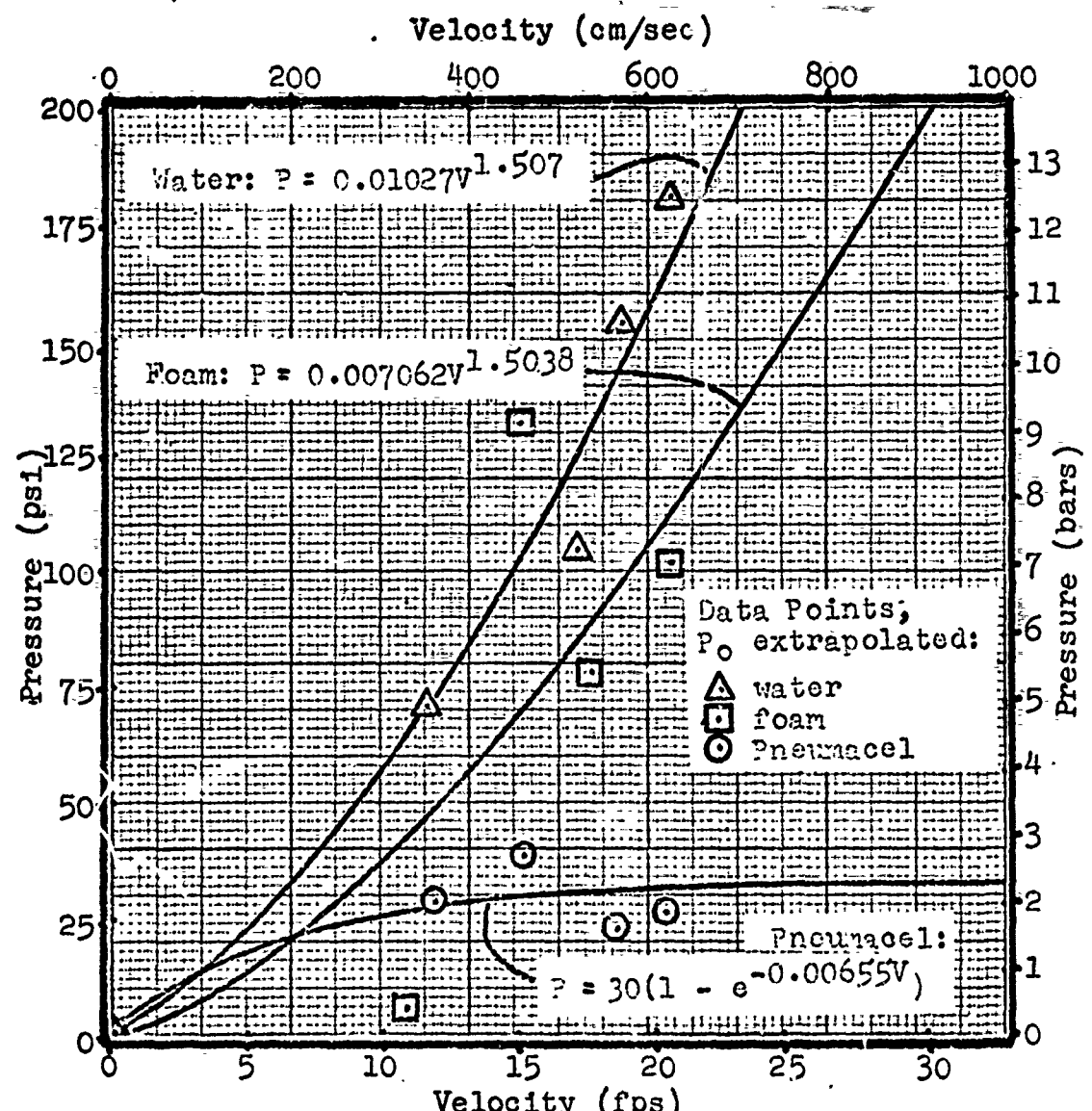


Figure 24

P₀ extrapolated vs Velocity

pressures than were measured in this study. Table III, Appendix C lists the theoretical pressures, densities, shock wave velocities, particle velocities, acoustic velocities, arrival times of the shock waves and rarefaction waves at the different gages, and the time and depth at which the rarefaction wave overtakes the shock wave.

Assuming values of P_0 as given in Table I obtained by extrapolating back to the surface are at least representative of the actual pressures, the Fowles model predicts pressures that average 8.3 times greater than experimental findings for water, 20.4 times greater for the water-foam mixture, and 2.13 times greater for the water-Pneumacel mixture. The simple mixture model used predicts that the water-foam mixture will be less compressible than water and therefore give higher pressures for the same impact velocity. The experimental results showed lower pressures for the water-foam mixture than for water, thus producing the great difference. The mass fractions used in the water-fcam calculations were based on manufacturer's data giving the volume fraction of the foam as 1.8%. Experimental measurements (results for all mixtures listed in Table IV, Appendix C) showed the volume fraction of the water was approximately 92%, revealing approximately 6% by volume air present. Computing the pressures considering 6% by volume air to be present in the water-foam mixture led to the predicted pressures an average of 2.36 times greater than the experimental findings. The remaining differences between experimental and theoretical values are likely due to the fact that P_0 was estimated

by extrapolation and due to trapped air providing some cushioning of the impact disc. Since the experiment was conducted in the air, a thin layer of air was likely trapped between the impact disc and the target material, decreasing the pressure generated by the impact.

Considering the water-foam mixture as a porous mixture with roughly the same percent volume of gas (6% air in the water-foam, and 7.8% Freon in the water-Pneumacel) led to the question of why the Pneumacel showed significantly greater attenuation than the water-foam target. Freon, with a gas constant of 1.12 is considerably more compressible than air. Theoretically the limiting compressibility of air is 6, while the same limit for Freon is 17.67, nearly 3 times greater. Thus the choice of Freon as the gas to be used in the mixture is important since for a given volume displaced it is capable of producing greater pressure attenuation. The significance of the compressibility is also shown in the theoretical calculations. Table III shows the depth at which the rarefaction wave overtakes the shock wave is hundreds of centimeters for water and for water-foam, but less than 1 cm for water-Pneumacel and water-foam-air.

The arrival time of the shock wave at the transducers was in good agreement with shock velocities calculated in water and the mixtures if the water-foam mixture were considered to be water-foam-air. The pressure rise in the water is very steep, approaching the step jump in pressure expected with a shock wave. However, in the water-foam and water-Pneumacel mixtures, the pressure pulse is less abrupt,

becoming quite diffused with distance in Pneumacel.

The air present in the water-foam mixture was included unintentionally in the form of bubbles trapped in foam cells. Most of the air would not have been trapped in the foam if fuel had been used instead of water because of increased wetting with fuel. Consequently the attenuation of pressures in a fuel-foam mixture can be expected to be much less than measured in the water-foam-air mixture.

Experiment II. Most models for projectile impacts into fluids, for example Yarkovich (Ref 12) considered that all of the kinetic energy of a projectile is deposited at the point of impact. This is not the case in general, and especially in Experiment II where the projectile was fired into the fluid through a thin Mylar film. When fully developed, models of the pressure field, such as those by Bristow (Ref 2) and Lundstrom (Ref 8) should be able to predict pressures in a ballistic experiment like the second part of this research.

In addition to the pressure generated by the impact, gage 3 sensed pressures generated by the projectile moving through the fluid. To look at the attenuation of the initial pressure pulse, it was necessary to see what pressures the gage recorded at the time the initial pulse should have reached it. This pressure was much less than the maximum pressure recorded by gage 3. Figures 25-27 show the plot of pressure versus distance for the three target materials for representative shots grouped as high, medium, and low impact velocities. Since only three data points are available, simple curve fits were used and no attempt was made to

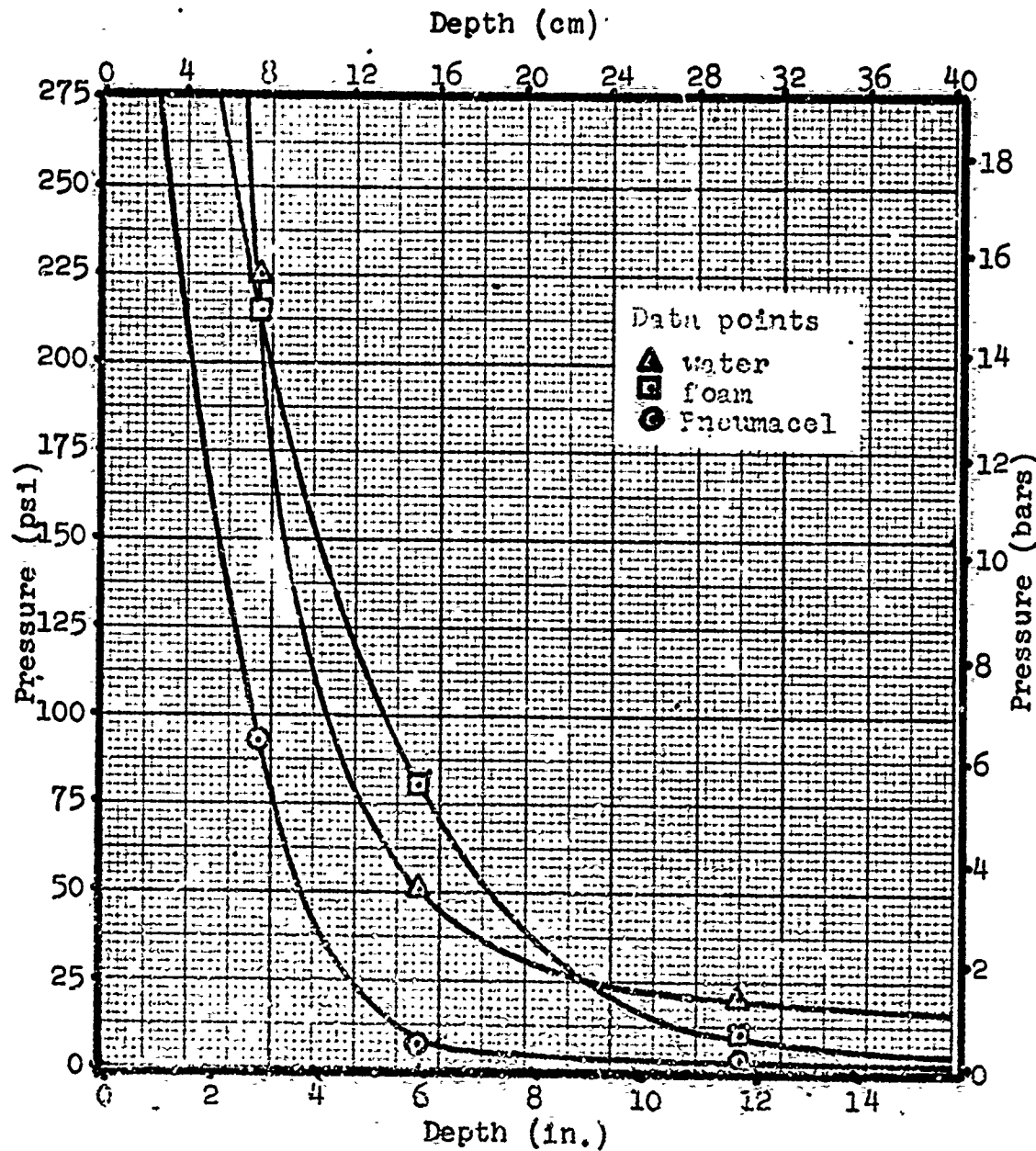


Figure 25

Pressure vs Depth,
Low Velocity Group,
Shots 11, 18, &
average of 5 & 14

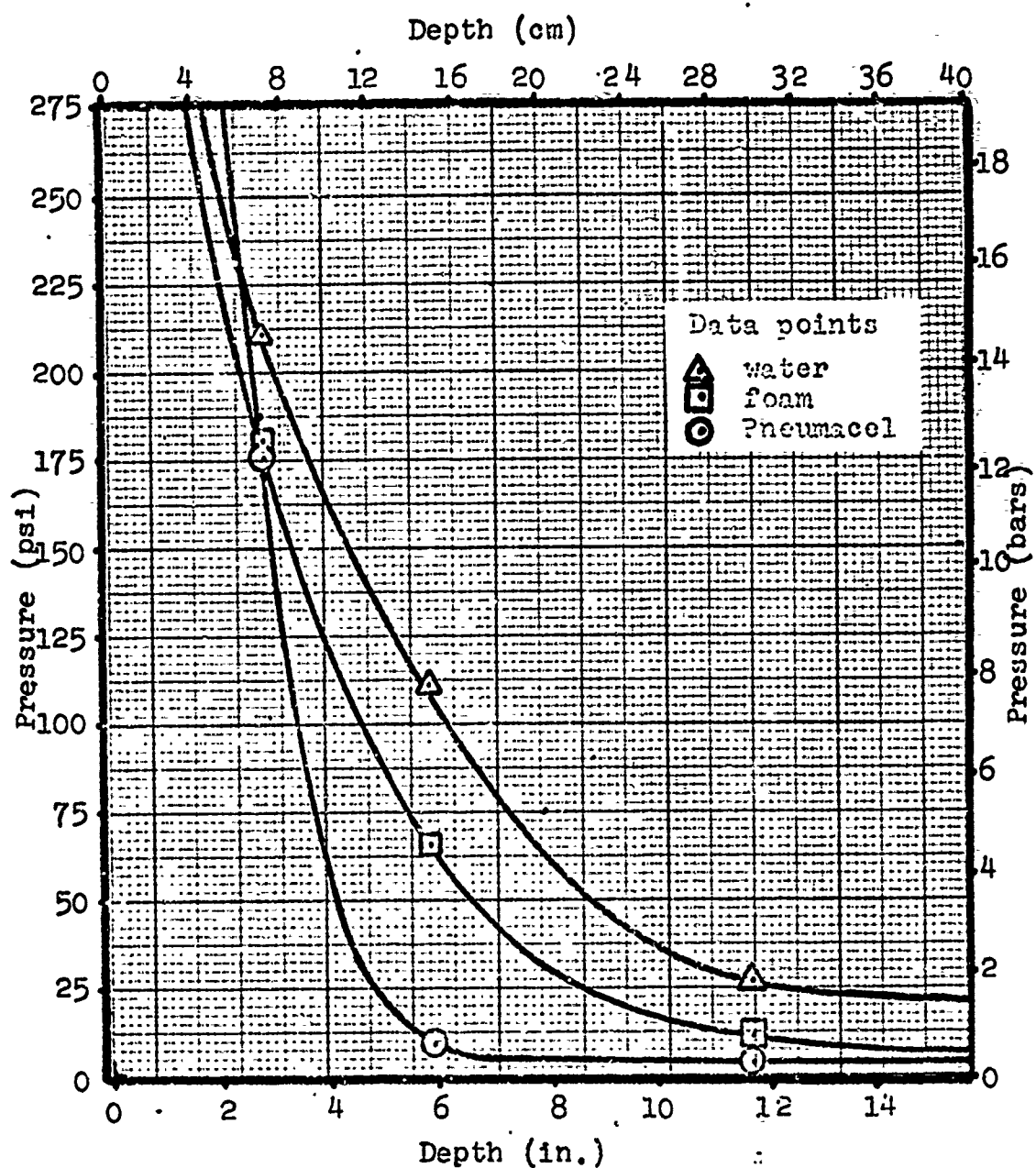


Figure 26
Pressure vs Depth,
Medium Velocity Group,
Shots 2, 6, 12

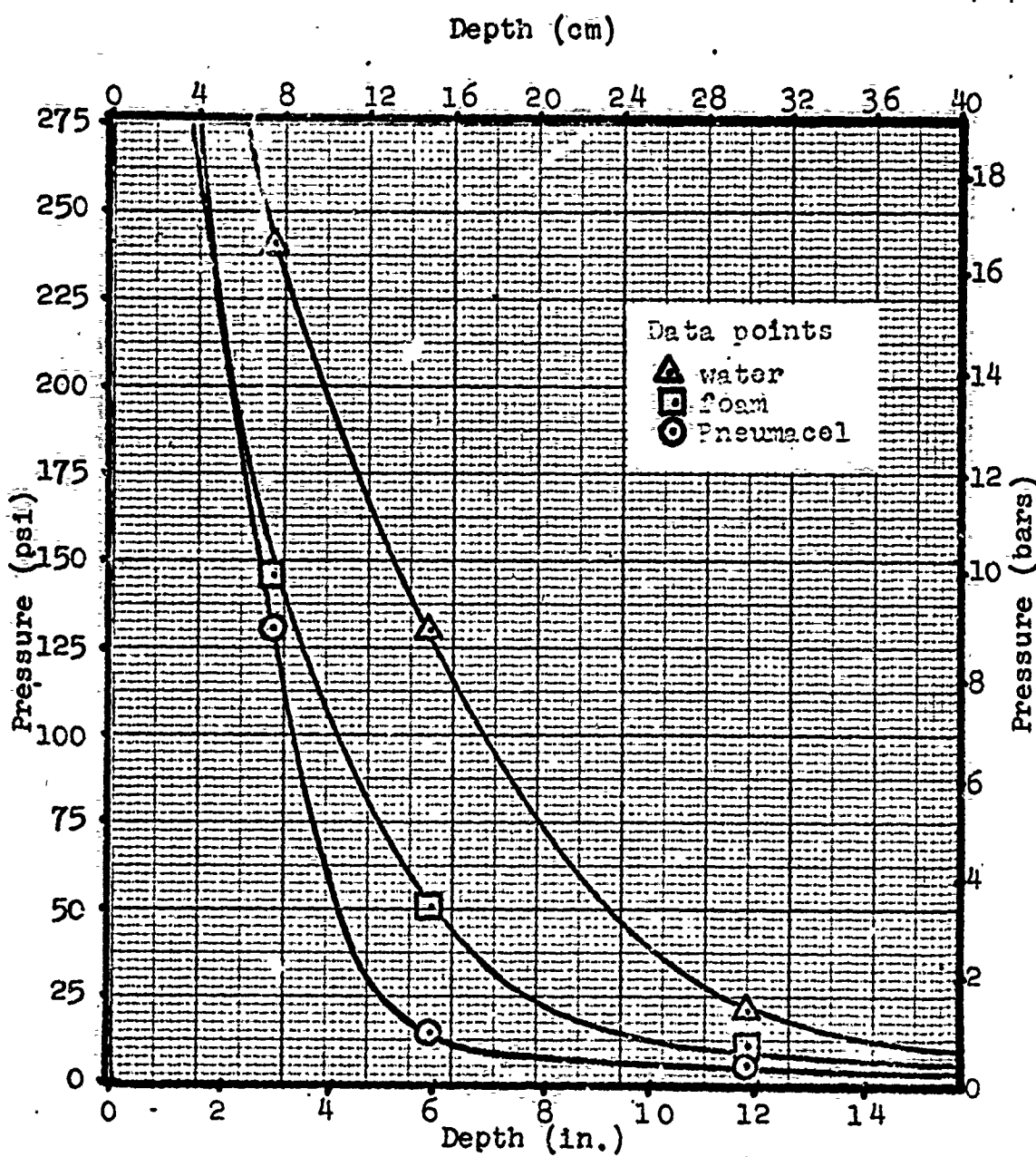


Figure 27

Pressure vs Depth

High Velocity Group

Shots 13, 16, 20

predict an extrapolated P_0 . Although a comparison between the two experiments cannot be made on a one to one basis, it should be noted that the depth and distance between gages 1 and 3 in Experiment I is the same as the depth and distance between gages 1 and 2 in Experiment II. Comparing pressures on this basis shows much greater attenuation in every case in Experiment II. This is to be expected since the shock wave attenuates by geometric divergence in addition to mechanical losses. Figure 28 shows the pressure versus distance for the highest drops of Experiment I and the low velocity group of Experiment II plotted together and shows the increased attenuation in Experiment II.

Many experimenters with hydraulic ram (Bristow and Lundstrom, for example) feel that the pressure field phase is the major damage causing mechanism. Since this is the major source of the pressure pulse recorded at gage 3, it is interesting to compare the magnitude of the readings of gage 3 in the three mixtures. Figure 29 plots the maximum pressure recorded at gage 3 versus the impact velocity. Pneumacel clearly attenuates the majority of the pressure generated by the moving projectile. As in Experiment I, the water-foam mixture is actually water-foam-air mixture, and the pressures shown are more attenuated than would be the case in a fuel-foam mixture where little air would be present. In Figure 29 the greater scatter of data points for the water-foam mixture is believed to be caused by the inhomogeneous nature of the air bubbles in the water-foam mixture.

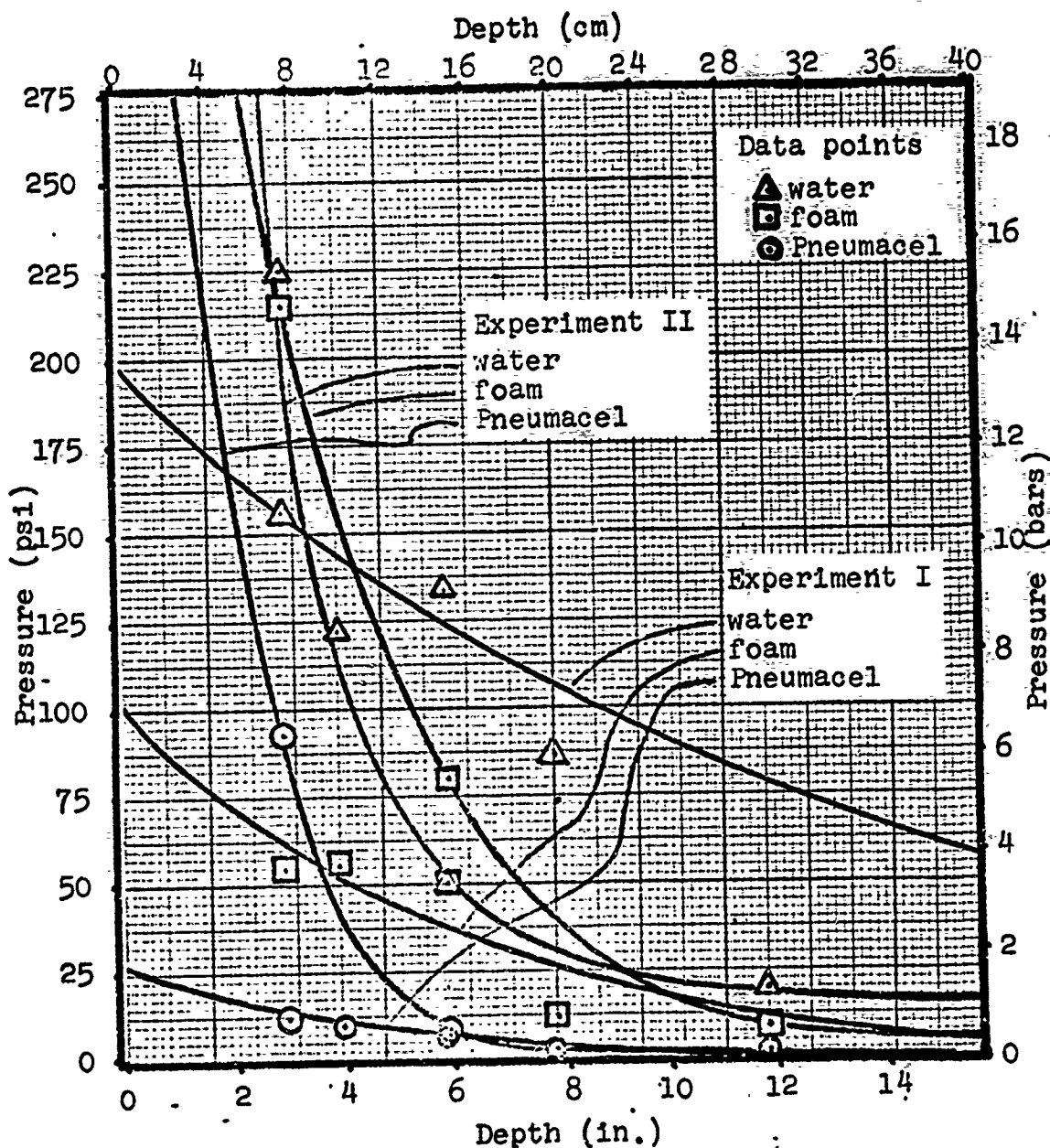


Figure 28

Pressure vs Depth

2 m Drops and Low Velocity Group

GAW/MC/72-3

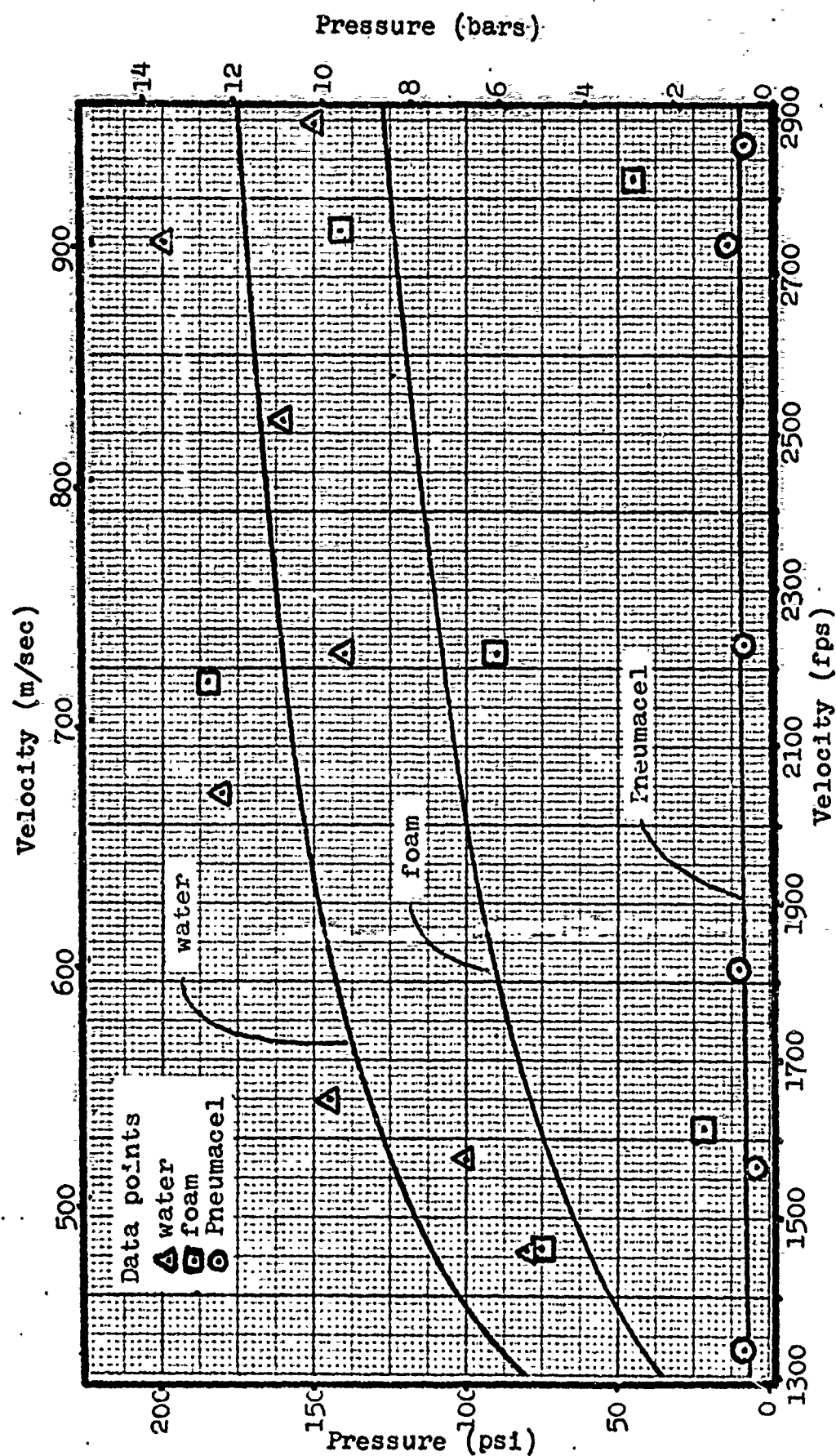


Figure 29, Impact Velocity vs Gage 3 Pressures

VI. Conclusions and Recommendations

Conclusions

1. Plane shock waves can be used to simplify the study of some aspects of the hydraulic ram phenomenon, such as the relative attenuation of materials.
2. Attenuation shown in plane shock wave experiments is less than the attenuation under similar circumstances for ballistic tests.
3. Including a small fraction of a gas in the fuel-foam mixture significantly reduces the magnitude of pressure pulses at any point and increases the attenuation of pressure pulses that are present.
4. The addition of reticulated polyurethane foam does not significantly increase the attenuation of shock waves. Since some air was known to be present in these experiments, the major attenuation factor is believed to be the air present.
5. Air is not the best gas to use for the purpose of increasing attenuation. Freon or another highly compressible gas produces greater attenuation for the volume it displaces.
6. The impact assembly used in Experiment I is not a satisfactory method of calibrating Kistler pressure transducers since the gages must be mounted some distance from the impact plane to protect them, and because the presence of an air cushion under the impact disc makes it difficult to predict exact pressures created by the impact.

Recommendations

1. Foams with a controlled amount of a gas should be included in future tests of hydraulic ram defenses.
2. Foams with various densities, various amounts of a gas, and various types of gases should be investigated to determine their efficiency in attenuating hydraulic ram type pressure pulses.
3. A foam should be designed which will combine the flame front supressing characteristics of reticulated polyurethane foam and the pressure attenuating characteristics of a gas-filled foam.
4. Fuel should be used in tests wherever possible to reduce the amount of air accidentally introduced into the experiment.
5. To decrease the volume of fuel sacrificed to foams, the efficiency of using layers of various thicknesses of gas-filled foam next to the fuel cell walls and no foam, or a lower density foam, in the center of the tank should be tested.

Bibliography

1. Blakemore, Colin B. personal correspondence to James W. Clark, Jr., (January 1972).
2. Bristow, R.J. "Approach to a Hydraulic Ram Fluid and Tank Wall Response Model." Aerospace Group, the Boeing Company, (July 1971).
3. Clark, G.O. "Gunfire Testing of a Rigid Fuel Container to Determine the Shock Attenuation Values of Foam." Report No. 2-59920/OR-8389. Dallas, Texas: Vought Aeronautics Division, LTV Aerospace Corporation, (August 1970).
4. Fischer, Richard F. "A Theoretical Investigation of Shock Waves in Water and Water-Polyurethane Foam Mixtures." M.S. Thesis, Air Force Institute of Technology, Wright-Patterson Air Force Base, Ohio, (June 1971).
5. Fowles, G.R. "Attenuation of the Shock Wave Produced in a Solid by a Flying Plate." Journal of Applied Physics, 31:655-661, (April 1960).
6. Heitz, R.M. "Self-sealing Systems for Integral Fuel Tanks." Northrop Corporation TR AFML TR-68-103, (June 1969).
7. Herrmann, W. "Constitutive Equation for the Dynamic Compaction of Ductile Porous Materials." Journal of Applied Physics, 40:2490-2499, (May 1969).
8. Lundstrom, Eric A. "Fluid Dynamic Analysis of Hydraulic Ram." NWC TP 5227, Naval Weapons Center, China Lake, California, (June 1969).

GAW/MC/72-3

9. Northrop Corporation, "Shock Wave Study." Unpublished paper.
10. Torvik, P.J. "A Simple Theory for Shock Propagation in Homogeneous Mixtures." Air Force Institute of Technology TR 70-3, (May 1970).
11. Williams, Roger F. "Shock Effects in Fuel Cells." Stanford Research Institute Project No. PGD 7708, Stanford Research Institute, (October 1969).
12. Yurkovich, R.W. "Hydraulic Ram: A Fuel Tank Vulnerability Study." McDonnell Report 6964. St. Louis: McDonnell Aircraft Corp., (September 1967).

Appendix A

Target Materials

Pneumacel

Pneumacel, shown in Figure 30, is a new Du Pont product now in pilot production. A small supply of Pneumacel was made available for this study by Mr. Colin B. Blakemore, Christina Laboratory, Wilmington, Delaware, 19898. The following information is also courtesy of Mr. Blakemore (Ref 1).

Batt Characteristics

Randomly oriented, thermoplastically bonded Pneumacel fibers.

Density: appx. 0.2 lbs/cu ft to appx. 3.5 lbs/cu ft.

Thickness: appx. 0.2 in, and up.

Chemical characteristics similar to:
polyvinyl acetate
fluorinated hydrocarbons
"Dacron" polyester fiber.

Fiber Characteristics

Small, uniform, polyhedral cells.

Thin, highly oriented cell walls.

Low density- appx. 0.023 gm/cu cm.
for individual strand which included 12%
by weight of an inert inflatant.

Compression strength: essentially undamaged
@ 3,000 psi.

Chemical properties similar to "Dacron" poly-
ester fiber and fluorinated hydrocarbon blow-
ing agents.

Adjustably pressurized (1-30 psig).

Note: Pneumacel in its present form is not recommended for

use in fuels because the fuel may soften the material used to bond the fibers into a mat.

Reticulated Polyurethane Foam

Figure 31 is a picture of the polyurethane foam used in this study.

Foam Characteristics

Appx. 15 pores per inch.

Density: 1.3 lbs/cu ft.

Volume fraction: 1.8%.

Retained fuel: 1.1%.



Figure 30 Pneumacel
Photograph is approximately to scale

Reproduced from
best available copy.

RETICULATED POLYURETHANE FOAM

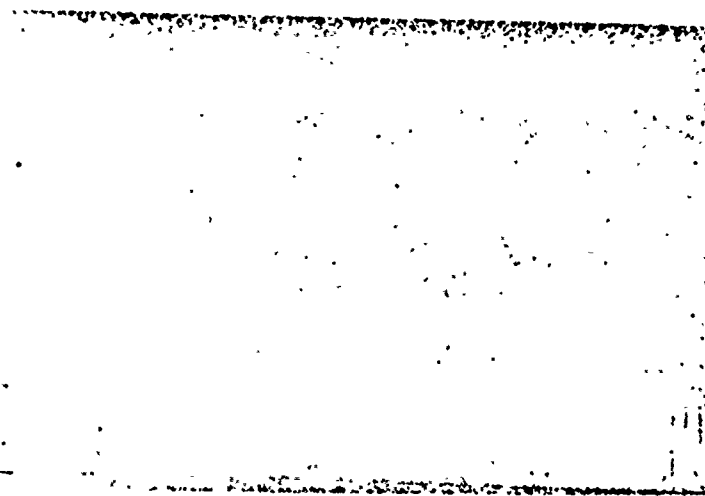


Figure 31
Reticulated Polyurethane Foam

Appendix B

Equipment Calibration

The Sangamo 3562 tape recorder was set in the FM record-playback mode and calibrated according to the technical manual. The output level was checked by recording a 1 KHz, 1 volt signal on each channel and checking the amplitude and wave form on an oscilloscope and Visicorder. A 25 KHz, 1 volt signal was also recorded and checked. This signal was 5 KHz beyond the recommended specifications of the tape recorder, but the wave form and voltage appeared good.

The Honeywell 1508 Visicorder Oscilloscope had six Honeywell M-3300 subminiature galvanometers installed, and the recorded reference signal was played on each channel for a systems check. The galvanometers have an undamped natural frequency of 3300 hz and flat response ($\pm 5\%$) from 0 to 2000 hz. The Visicorder specifications stipulate linear performance within $\pm 2\%$ for peak to peak deflections up to 6 in. Maximum peak to peak deflections encountered in the experiments were $2\frac{1}{2}$ in. The reference signal recorded with the data was played on each channel as a calibration prior to the final playback of data on the Visicorder.

The Kistler 603-A pressure transducers were calibrated for 1000 psi/volt and 100 psi/volt. All gages were simultaneously tested in a manifold made of 2 in. diameter steel pipe fittings (Figure 32) attached to a dead weight tester. The first two calibration drops were used to determine

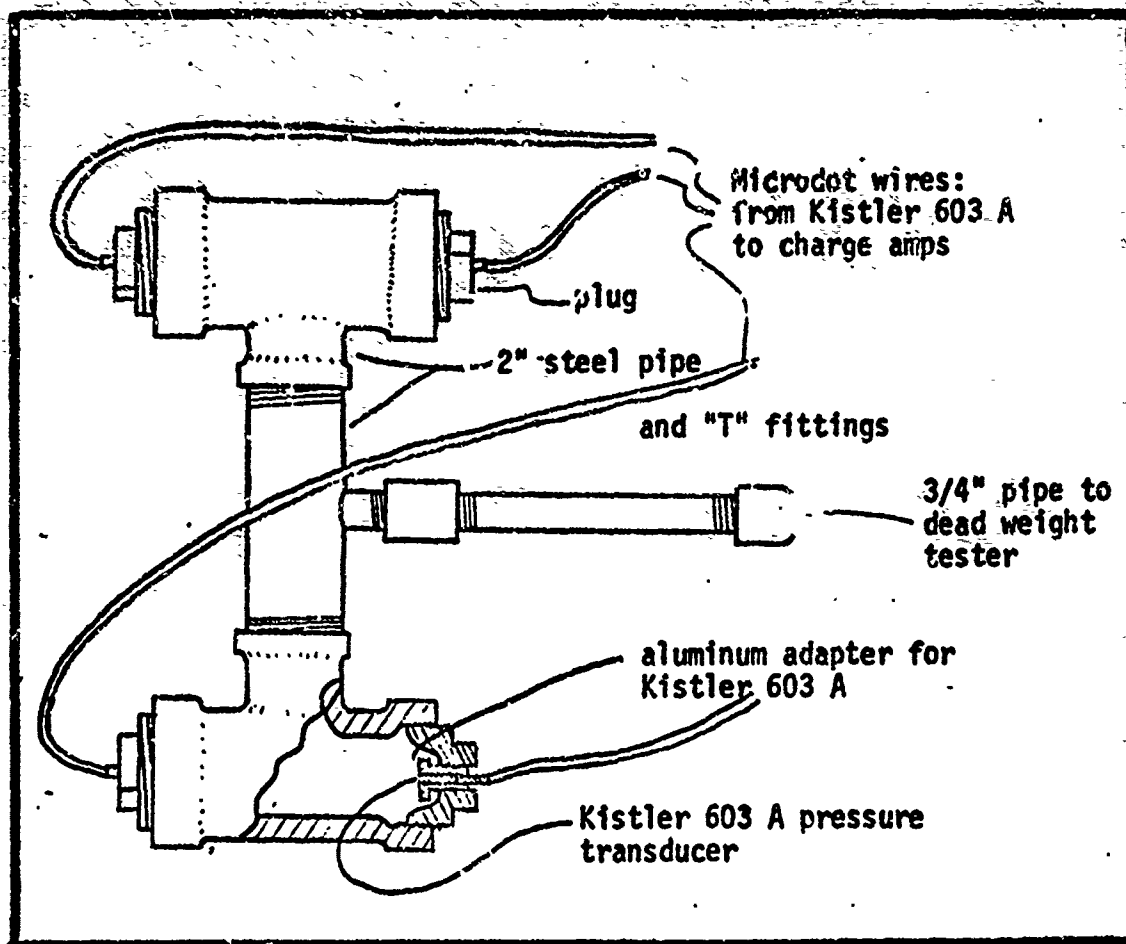


Figure 32
Pressure Calibration Apparatus

which calibration of the charge amplifiers gave the best results. The 1000 psi/volt setting proved too insensitive, so the 100 psi/volt setting was used throughout. Calibrating the Kistler system in accordance with the technical manual required static testing. The charge amplifiers were set to the long time constant setting and calibrated pressures from a dead weight tester were applied. This type calibration may or may not be accurate when the charge amplifiers have

GAW/MC/72-3

the short time constant setting and the gages measure very dynamic pressure pulses. However, the magnitude and shape of recorded pulses in the experiment were well within the range of results obtained by other researchers in the field, and the relative values should be accurate in any case.

Appendix C

Calculation in Support of Results
of Experiment I

Velocity of Impact Disc

To determine the impact velocity of the impact disc, the time required for the impact assembly to fall the distance between any two of the contact brushes was physically measured on the Visicorder film by comparing the initial contact points of the brushes with the recorded 1KHz reference signal. The results were tabulated and each drop was plotted on 10x15 in. graph paper. A smooth curve connecting the data points was extrapolated to 47, 54, and 54 cm points. The average velocity between any two data points was calculated by $v_{avg} = \Delta x / \Delta t$. To obtain the velocity at the impact point, $x=47$, the values from the extrapolated curve were used with $\Delta x = (x=54) - (x=40)$ and Δt taken from the same points. The velocity was also calculated for the points $x=5, 15, 25, 35, 43\frac{1}{2}$, and 45, to note the trend of the velocities as a check against large errors. Table II lists the results of the measurements and calculations and Figure 28 is a sample of the graphical solution used.

Theoretical Pressure Calculations

To determine the theoretical pressure at impact, three computer programs were used. In the first program, the Rankine-Hugoniot Equation and a linear Hugoniot equation of state for water and aluminum were solved simultaneously for the pressure, given the impact velocity and constants for

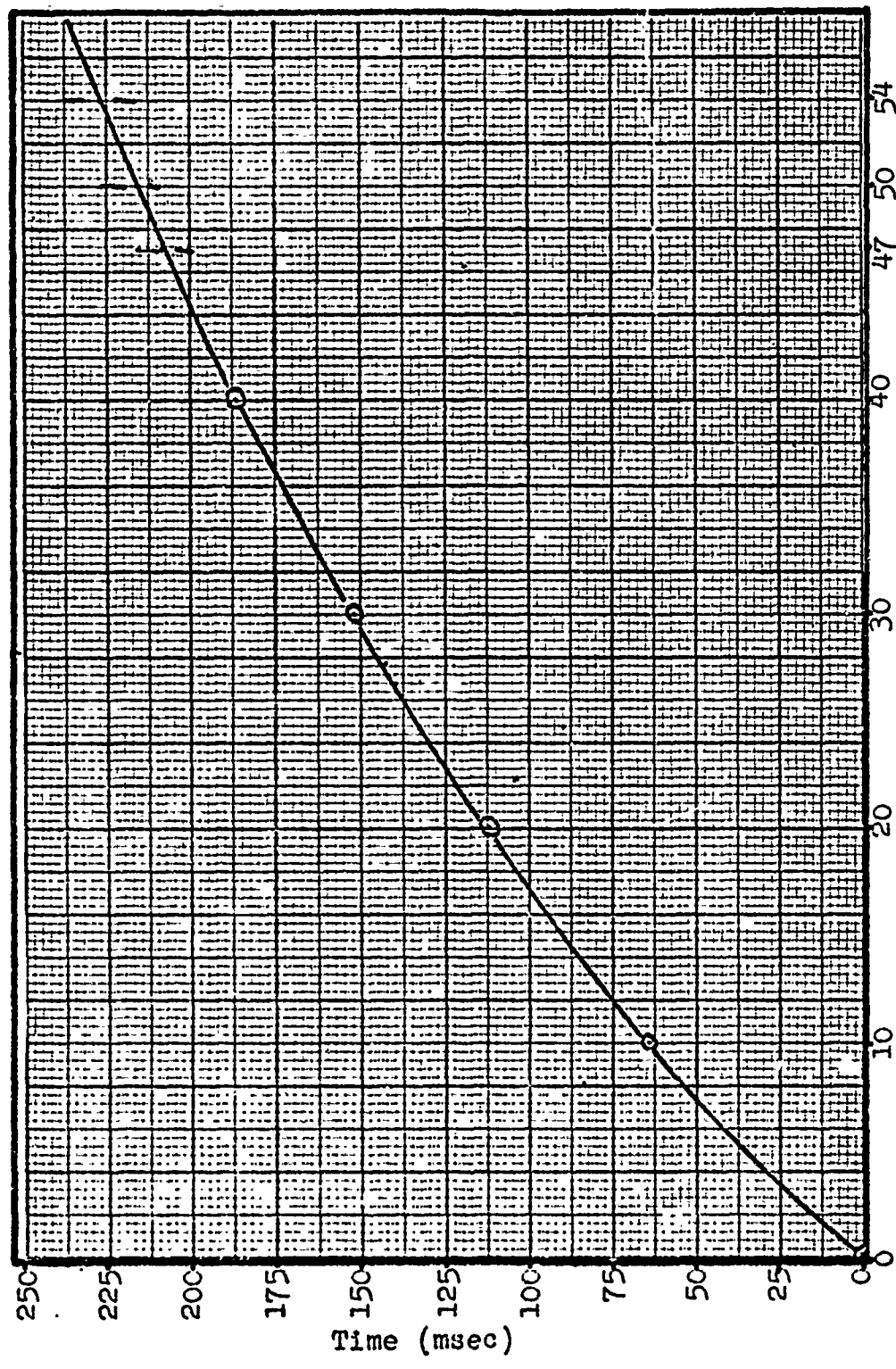


Figure 33
Example of a Graphical Solution of
Impact Velocity for Experiment I

Table II
Impact Velocity Calculations

Run	Δt_1 v_{1av}	Δt_2 v_{2av}	Δt_3 v_{3av}	Δt_4 v_{4av}	Δt_5 $v_{5av} \cdot 7$	Δt_6 $v_{6av} \cdot 10$	Δt_7 $v_{7av} \cdot 14$
5	64.0 156.2	48.0 208.2	40.0 250.0	34.5 290.0	21.0 333.3	30.0 333.3	40.0 350.0
6	28.6 349.8	26.7 374.2	25.7 389.2	22.9 437.0	14.0 500.0	19.3 518.0	26.9 520.0
7	21.3 470.0	20.7 483.0	19.8 504.0	19.0 526.0	12.7 551.0	18.0 556.0	24.7 557.0
8	17.75 564.0	17.3 578.0	16.7 598.0	16.4 610.0	11.65 601.0	16.25 616.0	22.6 619.0
9	64.2 155.8	47.5 210.7	39.4 254.0	34.6 289.0	21.3 328.8	29.0 345.0	38.8 360.8
11	28.5 351.0	26.4 379.0	24.9 402.0	23.5 426.0	15.6 448.0	21.8 459.0	30.3 462.0
12	21.3 470.0	20.6 486.0	19.8 505.0	19.1 524.0	12.8 547.0	17.9 558.0	24.8 564.0
13	17.7 565.0	17.3 578.0	16.75 596.5	16.3 612.5	11.6 604.0	16.25 615.0	22.7 617.0
14	65.8 152.7	53.5 227.5	34.5 227.5	34.8 287.2	21.5 325.0	31.0 323.0	42.6 329.0
15	28.5 351.0	26.6 376.0	24.9 401.5	23.7 422.0	15.4 454.0	21.8 458.0	30.4 461.0
16	42.1 476.0	42.1 476.0	19.8 505.0	19.1 523.5	13.0 538.0	18.6 538.0	26.0 539.0
17	17.7 565.0	17.2 582.0	16.8 595.0	16.3 613.0	11.5 610.0	16.1 621.0	22.5 622.0

the linear Hugoniot equation of state for each material. The particle velocities (U), shock velocities (D), and densities (ρ) were found for both water and the aluminum disc. The speed of sound (C) in the materials was calculated from the expression $C = \sqrt{\frac{dp}{d\rho}}$, where $\frac{dp}{d\rho}$ was solved from the expression of density as a function of pressure. Once these variables were calculated, the time of arrival of the initial shock wave and the first rarefaction wave at each pressure gage, and the depth the shock wave would travel before attenuation begins were calculated using the solution by Fowles (Ref 5). To obtain the same information for target mixtures, the simple mixture theories by Torvik (Ref 10) were used to calculate the average density of the mixtures as a function of pressure and mass fraction of the constituents and this program inserted into the previous program to calculate pressures, particle velocities, and shock speed. In this case, the program iterated pressures until a solution was found satisfying the conditions of the given impact velocity and the linear Hugoniot data for the aluminum plate. Once the impact pressure was determined, the program calculated the acoustic velocity in the mixture and the arrival times for shock waves and rarefaction waves as before. For a more complete discussion of the simple mixture theories and the Fowles model, see Fischer (Ref 4). An explanation of all terms used in Table III appears at the end of the table.

The mass fractions required in the previous calculations were determined by weighing the various constituents of the

GAW/MC/72-3

target mixtures on a beam balance and from manufacturers' data on the foams. The results are shown in Table IV.

Table III
Theoretical Calculations for Experiment I

Run	Mat'l	V ₁ cm/sec fps	P bar psi	ρ ₀ gm/cc	ρ cm/sec	D cm/sec 10 ⁻⁶	U cm/sec	C cm/sec 10 ⁻⁶	Theoretical Calculations for Experiment I			
									T ₁ TR ₁ msec	T ₂ TR ₂ msec	T ₃ TR ₃ msec	T ₄ TR ₄ msec
5	Water	350.0	47.25	1.000	1.002	.1490	317.6	.1493	.0503	.0671	.1007	.1343
	Al.	11.46	686.0	2.785	2.785	.5241	32.42	.5241	.0574	.0741	.1076	.1411
6	Water	520.0	70.50	1.003	.1493	471.7	.1498	.0502	.0670	.1005	.1340	.1453
	Al.	17.5	1021.0	2.785	.5241	48.25	.5241	.0571	.0738	.1071	.115	.217.0
7	Water	567.0	76.85	1.003	.1494	514.4	.1500	.0502	.0669	.1004	.1070	.1339
	Al.	18.59	1114.0	2.785	.5241	52.64	.5241	.0570	.0737	.1070	.1403	.199.3
8	Water	619.0	83.90	1.004	.1495	561.5	.1501	.0502	.0669	.1003	.1338	.1.223
	Al.	20.14	1217.0	2.785	.5241	57.51	.5242	.0569	.0736	.1069	.1402	.182.9
9	Pneu.	360.8	2.881	.8515	.9364	.0061	359.5	.0074	1.227	1.636	2.451	3.272
	Al.	11.83	41.85	2.785	.5240	1.281	.5240	1.021	1.358	2.032	2.706	.0432
11	Pneu.	462.0	3.53	.9462	.0064	460.3	.0090	1.164	1.552	2.328	3.104	.2640
	Al.	15.13	51.3	2.785	.5240	1.729	.5240	.8460	1.125	1.682	2.240	.0291
12	Pneu.	564.0	4.28	.9540	.0068	561.8	.0107	1.096	1.461	2.191	2.921	.1876
	Al.	18.50	62.2	2.785	.5240	2.243	.5240	.7080	.9407	1.406	1.872	.0234

Table III (continued)

Rn	Mat:1	V_1	P	ρ_0	ρ	D	U	C	T_1	T_2	T_3	T_4	TI3
		cm/sec	bar	gm/cc	gm/cc	cm/sec	cm/sec	cm/sec	TR1	TR2	TR3	TR4	msec Xmax cm
		fps	psi			10	10	10	msec	msec	msec	msec	
13	Pneu.	617.0	4.71	.8515	.9574	.0071	614.5	.0118	1.060	1.413	2.120	2.827	.0215
	A1.	20.22	68.4	2.785	.5240	2.536	.5240	.6480	.8607	1.286	1.712	.1524	
14	Foam	329.0	45.3	1.006	1.008	.1513	297.9	.1516	.0496	.0661	.0991	.1322	2.638
	A1.	10.79	657.8	2.785	2.785	.5241	31.1	.5240	.0592	.0757	.1087	.1417	382.1
15	Foam	461.0	63.6	1.008	.1515	417.4	.1519	.0495	.0660	.0990	.1320	1.887	
	A1.	15.12	922.9	2.785	.5241	43.6	.5240	.0591	.0755	.1085	.1414	.1414	285.9
16	Foam	539.0	74.4	1.009	.1517	488.0	.1521	.0495	.0659	.0989	.1319	1.616	
	A1.	17.68	1079.9	2.785	.5241	51.0	.5240	.0590	.0755	.1083	.1412	.1412	245.1
17	Foam	622.0	86.0	1.009	.1518	563.1	.1523	.0494	.0659	.0988	.1377	1.403	
	A1.	20.40	1247.3	2.785	.5241	58.9	.5240	.0589	.0754	.1082	.1410	.1410	212.9
14	F*air	329.0	4.52	.9461	.9825	.0114	326.6	.0191	.6610	.8813	1.322	1.763	.0230
	A1.	10.79	65.6	2.785	2.785	.5240	2.40	.5240	.4030	.5341	.7963	1.059	.2606
15	F*air	461.0	6.67	.9866	.0131	457.1	.0275	.5723	.7630	1.145	1.526	.0179	
	A1.	15.12	97.0	2.785	.5240	3.90	.5240	.2823	.3732	.5550	.7367	.2352	

Table III (Continued)

Rn	Mat'1	V ₁ cm/sec fps	P bar psi	P _o gm/cc	P cm/sec 10 ⁶	D cm/sec 10 ⁶	U cm/sec 10 ⁶	C cm/sec 10 ⁶	T ₁ TR ₁ msec	T ₂ TR ₂ msec	T ₃ TR ₃ msec	T ₄ TR ₄ msec	T _{I3} X _{max} cm
16	F-air	539.0	8.21	.9461	.9883	.0143	534.1	.0334	.5251	.7015	1.052	1.403	.0165
	Al.	17.68	119.2	2.785	2.785	.5240	4.935	.5240	.2346	.3095	.4595	.6088	.2347
17	F-air	622.0	10.07	.9897	.0155	615.8	.0402	.4827	.6436	.9654	1.287	.0154	
	Al.	22.40	146.1	2.785	.5240	6.201	.5240	.1963	.2585	.3829	.5073	.2396	

Explanation of terms:

- Rn: Run number
 Mat'1: Materials (mixtures)
 V₁: Impact velocity
 P: Pressure calculated by Fowles theory
 P_o: Density of uncompressed materials
 P: Density of compressed materials
 D: Velocity of shock wave
 U: Particle velocity in compressed material
 C: Speed of sound in compressed material
 T_{1,2,3,4}: Arrival time of shock wave at gage 1,2,3,4 respectively
 TR_{1,2,3,4}: Arrival time of rarefaction wave at gage 1,2,3,4 respectively
 TI3: Time rarefaction wave overtakes shock wave
 X_{max}: Depth at which rarefaction wave overtakes shock wave

Table IV
Mass Fraction Calculations

Material	weight (oz)	Mass Fraction	Volume Fraction
total water	188.1		
water	173.5		
foam	4.7		
water-foam	178.2		
f_{mw} f_{mf} (2 part mixture)		.973625 .026375	
f_{vw} f_{vf} (3 part mixture) f_v air			.922381 .0180 .059619
f_{mw} f_{mf} (3 part mixture) f_{mg}		.923625 .026289 .000077	
water	162.3		
Pneumacel	1.5		
water-Pneumacel	163.8		
f_{mw} f_m Pneu. (12% Freon) f_{mf} f_{mg}		.990843 .009157 .008058 .001099	
f_{vw}			.862838

Appendix D

Tabulation of the maximum pressures and impact velocities of Experiment I and II follow. In Table VI, P_3' is the approximate value of the initial pressure pulse at gage 3.

Table V
Tabulated Results of Experiment I

Run	Impact Velocity	Appx. Height		x=7.5 cm		P ₁		P ₂		x=10 cm		P ₃		x=15 cm		P ₄		x=20 cm	
		cm/sec	fps	m	ln.	bar	psi	bar	psi	bar	psi	bar	psi	bar	psi	bar	psi	bar	psi
5W*	350	11.48	$\frac{1}{2}$	19.7	2.27	33	1.653	24	1.106	16	.620	9							
6W	520	17.05	1	39.4	4.41	64	3.24	47	2.148	36	1.86	27							
7W	567	18.55	$1\frac{1}{2}$	59	7.64	111	5.78	84	5.37	78	3.92	57							
8W	619	20.3	2	78.8	10.74	156	8.40	122	9.16	133	5.99	87							
9P	360.8	11.82	$\frac{1}{2}$	19.7	.551	8	.274	4	.1378	2	.1378	2							
11P	462	15.11	1	39.4	.689	10	.274	4	.206	3	.1378	2							
12P	564	18.49	$1\frac{1}{2}$	59	1.032	15	.827	12	.827	12	.482	7							
13P	617	20.23	2	78.8	.827	12	.689	10	.551	8	.1378	2							
14F	329	10.79	$\frac{1}{2}$	19.7	.758	11	.689	10	1.171	17	.413	6							
15F	461	15.12	1	39.4	4.54	66	2.685	39	3.03	44	.689	10							
16F	539	17.7	$1\frac{1}{2}$	59	3.03	44	1.99	29	2.54	37	.482	7							
17F	622	20.4	2	78.8	3.72	54	3.79	55	3.44	50	.827	12							

*W:water, P:Pneumacel, and F:foam.

Table VI

Tabulated Results of Experiment II

Run	Impact Velocity m/sec fps	P ₁ r=7.5 cm bar psi	P ₂ r=15 cm bar psi	P ₃ r=30 cm bar psi	P' ₃ r=30 cm bar psi
1W	480 1571	14.48 210	5.52 * 80 *	5.89 100	0.69 10
2W	677 2219	14.48 210	7.58 * 110 *	9.65 140	1.72 25
3W	767 2516	14.48 210	5.52 * 80 *	11.02 160	2.75 40
4W	884 2896	16.90 245	6.89 * 100 *	10.33 150	2.75 40
5P	477.5 1566	9.65 140	0.41 * 6 *	0.28 4	0.14 2
6P	681 2230	12.06 175	0.55 * 8 *	0.55 8	0.14 2
7P	875 2869	10.68 155	** **	0.55 8	0.14 2
8F	492 1612	12.06 175	** **	1.52 22	0.69 10
9F	677 2219	12.76 185	** **	6.21 90	1.03 15
10F	862.5 2823	14.48 210	** **	3.10 45	1.38 20
11F	446 1460	14.82 215	5.52 80	5.17 75	0.69 10
12F	665 2180	12.41 180	4.48 65	12.76 185	0.69 10
13F	842 2759	10.0 145	3.44 50	9.79 142	0.69 10
14P	407 1333	3.10 45	0.55 8	0.55 8	0.34 5
15P	554 1816	9.65 140	0.69 10	0.69 10	0.34 5
16P	836 2740	8.97 130	0.97 14	0.95 14	0.34 5
17W	504 1650	16.52 240	4.48 65	10.00 145	1.38 20
18W	445 1459	15.50 225	3.44 50	5.52 80	1.38 20
19W	662 2040	14.48 210	7.24 105	12.41 180	1.38 20
20W	839 2747	16.52 240	8.07 130	13.79 200	1.38 20

*Data questionable

**No data

†W: water, P: Pneumacel, and F: foam

Vita

James Walker Clark, Jr. was born April 12, 1938 in San Jose, California. After graduation from Fairborn High School, Fairborn, Ohio, in 1956, he entered the Air Force Academy. He was graduated in 1960 with a Bachelor of Science degree in Engineering Science and was commissioned in the United States Air Force. Following graduation from pilot training at Williams Air Force Base, Arizona, in September 1961, he flew: F-102 aircraft at Perrin Air Force Base, Texas, and Richards-Gebaur Air Force Base, Missouri, and at Goose Air Base, Labrador; F-106 aircraft at Tyndall Air Force Base, Florida, McChord Air Force Base, Washington, and at Osan Air Base, Korea; O-1 (FAC) in South Vietnam.

He attended Squadron Officers' School, Maxwell Air Force Base, Alabama, in 1964. He is a member of Tau Beta Pi National Engineering Honor Society.

Permanent address: 1934 Hawaii Ave. N.E.

St. Petersburg, Florida 33703